AD 748 191

Reproduced by
NATIONAL TECHNICAL
INFORMATION SERVICE
U S Department of Commerce
Springfield VA 22151

UNCLASSIFIED

Security Classification

## DOCUMENT CONTROL DATA - R & D

*Security classification of title, body of abstract and indexing annotation must be entered when the overall report is classified)*

1. ORIGINATING ACTIVITY (Corporate author)

School of Engineering
University of Massachusetts
Amherst, Massachusetts 01002

2a. REPORT SECURITY CLASSIFICATION

UNCLASSIFIED

2b. GROUP

3. REPORT TITLE

INFLUENCE OF TRANSVERSE SHEAR AND TRANSVERSE NORMAL STRESS ON LARGE DEFLECTIONS OF ORTHOTROPIC ARCHES

4. DESCRIPTIVE NOTES (Type of report and inclusive dates)

5. AUTHOR(S) (First name, middle initial, last name)

Michael Y. H. Hsu and William A. Nash

6. REPORT DATE

April 1972

7a. TOTAL NO. OF PAGES

52 + ix

7b. NO. OF REFS

24

8a. CONTRACT OR GRANT NO.

ONR-N00014-68-A-0146-

b. PROJECT NO.

In House Project Number

c. N00014-68-A-0146-16

d.

9a. ORIGINATOR'S REPORT NUMBER(S)

UM-72-4

9b. OTHER REPORT NO(S) (Any other numbers that may be assigned this report)

10. DISTRIBUTION STATEMENT

APPROVED FOR PUBLIC RELEASE; DISTRIBUTION UNLIMITED

11. SUPPLEMENTARY NOTES

12. SPONSORING MILITARY ACTIVITY

Department of Defense (ONR)

13. ABSTRACT

The problem of finite-amplitude deflections of a thin, elastic, shallow arch subject to uniform normal pressure is considered. A composite-material arch is investigated wherein closely spaced glass reinforcing elements in the form of extremely small diameter rods are oriented normal to the arch middle surface and bonded into an epoxy matrix. Transverse shear and transverse normal stress effects are included, as well as initial geometric imperfections in the structure. The governing equations are derived and solved by several approximate techniques to yield load-deflection characteristics from which buckling loads are obtained. The analytical results are confirmed through a series of experiments conducted on such arches.

DD FORM 1 NOV 65 1473 (PAGE 1)

S/N 0101-807-6811



UNCLASSIFIED

Security Classification

A-31408

UNCLASSIFIED

Security Classification

| KEY WORDS | LINK A | | LINK B | | LINK C | |
|---|---|---|---|---|---|---|
| | ROLE | WT | ROLE | WT | ROLE | WT |
| Arches | | | | | | |
| Orthotropic | | | | | | |
| Transverse Shear | | | | | | |
| Buckling | | | | | | |
| Structure | | | | | | |

DD FORM 1 NOV 65 1473 (BACK)

S/N 0101-807-6921



UNCLASSIFIED

Security Classification

A-31409

# INFLUENCE OF TRANSVERSE SHEAR AND TRANSVERSE NORMAL STRESS ON LARGE DEFLECTIONS OF ORTHOTROPIC ARCHES

By

Michael Y. H. Hsu and William A. Nash

Contract No. ONR-N00014-68-A-0146-16
Report No. UM-72-4

APPROVED FOR PUBLIC RELEASE; DISTRIBUTION UNLIMITED

D D C
RECEIVED
SEP 13 1972
B

April 1972

Approved for Release

Reproduction in whole or in part is permitted for any purpose of the United States Government. This research was sponsored by the Office of Naval Research under ONR Contract No. N00014-68-A-0146, Subcontract No. N00014-68-A-0146-16, ONR Contract Authority Identification No. NR 200-016.

Joseph M. Colonell
Joseph M. Colonell
Contract Manager
University of Massachusetts

## ACKNOWLEDGMENT

This study was supported by the Department of the Navy, Office of Naval Research, Contract ONR-N00014-68-A-0146-16. The authors wish to express their thanks for this support.

# TABLE OF CONTENTS


| | | Page |
|---|---|---|
| ABSTRACT | | iii |
| ACKNOWLEDGMENT | | iv |
| TABLE OF CONTENTS | | v |
| LIST OF FIGURES | | vii |
| NOMENCLATURE | | viii |
| Section | | |
| I | INTRODUCTION | 1 |
| II | CLASSICAL THEORY | 4 |
| | II.1 Introduction | 4 |
| | II.2 Strain-Displacement, Stress-Strain Relations | 5 |
| | II.3 Derivation of Equilibrium Equations and Natural Boundary Conditions | 7 |
| | II.4 Solution to the Equations | 9 |
| | II.5 Discussion of Results | 13 |
| III | TRANSVERSE SHEAR DEFORMATION AND TRANSVERSE NORMAL STRESS THEORY TOGETHER WITH A CONSIDERATION OF INITIAL IMPERFECTIONS | 21 |
| | III.1 Introduction | 21 |
| | III.2 Strain-Displacement Relations | 22 |
| | III.3 Derivation of Stress-Strain Relations and Equilibrium Equations | 23 |
| | III.4 Non-dimensionalized Equations | 27 |
| | III.5 Comparison of Three Theories | 31 |
| | III.6 Method of Solution | 32 |
| | III.7 Discussion of Results | 33 |
| IV | EXPERIMENTS ON RADIALLY REINFORCED ARCHES | 40 |
| | IV.1 Introduction | 40 |
| | IV.2 Fabrication of the Material | 40 |

TABLE OF CONTENTS (cont.)


| Section | | Page |
|---|---|---|
| | IV.3 Description of Test Apparatus . . . . . | 41 |
| | IV.4 Test Procedure . . . . . | 46 |
| | IV.5 Test Results . . . . . | 46 |
| V | CONCLUSIONS . . . . . | 50 |
| REFERENCES . . . . . | | 51 |

# LIST OF FIGURES


| Figure | | Page |
|---|---|---|
| 1 | (a) Coordinate System and Geometry . . . . . | 6 |
| | (b) Arch Element . . . . . | 6 |
| 2 | Load-Deflection Curve for Symmetric and Asymmetric Solutions for Hinged Ends . . . . . | 14 |
| 3 | Load-Deflection Curves for Clamped Ends . . . . . | 15 |
| 4 | Load-Deflection Curves for the Hinged Ends . . . . . | 16 |
| 5 | Load-Deflection Curves for the Clamped Ends . . . . . | 17 |
| 6 | Curves for Various Solutions - Hinged Ends . . . . . | 18 |
| 7 | Curves for Sym. and Asym. Solutions - Clamped Ends . . . . . | 19 |
| 8 | Load-Deflection Curves for Various Theories . . . . . | 34 |
| 9 | Comparison of Various Theories . . . . . | 35 |
| 10 | Upper Portion of Load-Deflection Curves . . . . . | 37 |
| 11 | Load Deflection Curves for Moderately Thick Arch . . . . . | 38 |
| 12 | Comparison Between Classical and General Theories . . . . . | 39 |
| 13 | (a) Sample of Radial Filament Arch with Clamped Supports . | 42 |
| | (b) The Arch Assembly and the Data Recording System . . . . | 42 |
| | (c) Testing Arch at Atmospheric Pressure . . . . . | 42 |
| | (d) Testing Arch at 165 p.s.i. Pressure . . . . . | 42 |
| 14 | Linear Variable Differential Transformer and Circuitry | 44 |
| | (a) Linear Variable Differential Transformer Consists of 3 Winding Transformers and a Core . . . . . | 44 |
| | (b) Additional Circuitry to Make Interpretation Easier . . | 44 |
| 15 | Comparison Between Theoretical and Experimental Results . . | 48 |
| TABLE 1 | Experimental Records . . . . . | 47 |

# NOMENCLATURE

| | |
|---|---|
| $A$ | Span of the arch |
| $E_x$(or $E$), $E_z$ | Young's moduli |
| $G$ | Shear modulus |
| $H$ | Rise of the arch |
| $h$ | Thickness of the arch |
| $L$ | Arc length of the arch |
| $M$ | Moment resultant |
| $N$ | Stress resultant |
| $\tilde{N}$ | Number of the grid point on the arch used in numerical analysis |
| $q$ | Uniformly distributed transverse load |
| $q_c$ | Critical uniformly distributed transverse load |
| $\bar{q}$ | $= q/E_x$ |
| $Q$ | Nondimensional load $= qL^4/E_x h^4$ |
| $Q_c$ | $= q_c L^4/E_x h^4$ |
| $R$ | Radius of curvature of middle surface |
| $S$, $T$ | Force resultants contributing to the transverse normal stress |
| $U$ | Tangential displacement component at an arbitrary point |
| $U_b$ | Bending strain energy |
| $U_m$ | Membrane strain energy |
| $U_o$ | Strain energy density |
| $U_t$ | Strain energy of entire arch |
| $u$ | Tangential component of displacement of the middle surface |
| $u'$ | Change of slope of the normal to the middle surface |
| $W$ | Radial displacement component at an arbitrary point |

| | |
|---|---|
| $w$ | Radial component of displacement at the middle surface |
| $w_c$ | $w$ at the mid-point of the arch |
| $w'$, $w''$ | Elements of power series expansion of $W$, contribution to the transverse normal strain |
| $w_o$ | Initial radial imperfection |
| $w_{oo}$ | Amplitude of initial radial imperfection |
| $\bar{w}_o$ | $= w_o/h$ |
| $\bar{w}_{oo}$ | $= w_{oo}/h$ |
| $x$ | Coordinate extending from one end of the arch along the middle surface |
| $z$ | Coordinate of an arbitrary point measured along the outward normal to the middle surface |
| $\alpha$ | $= w/h$ |
| $\alpha'$ | Angle of extension of the arch |
| $\beta$ | $= (L/h)\cdot w'$ |
| $\gamma$ | $= (L^2/h)\cdot w''$ |
| $\delta_s$ | Central difference operator |
| $\varepsilon_x$, $\varepsilon_z$ | Components of direct strain |
| $\gamma_{xz}$ | Component of shearing strain |
| $\sigma_x$, $\sigma_z$ | Component of direct stress |
| $\tau_{xz}$ | Component of shearing stress |
| $\nu_{xz}$, $\nu_{zx}$ | Poisson's ratios |
| $\lambda$ | $= L^2/Rh$ (Geometric arch parameter) |
| $\Omega$ | Potential energy due to external load |
| $\Pi$ | Total potential energy |
| $\phi$ | $= (L/h^2)\cdot u$ |
| $\psi$ | $= (L/h)\cdot u'$ |
| $\alpha_{,x}$ | $= \frac{d\alpha}{dx}$ |

# CHAPTER I

# INTRODUCTION

The shallow arch represents one of the simplest realistic structures from which many of the features of elastic instability theory can be illustrated. As a result of this simplicity the various existing theories which have been proposed to describe the behavior of an arch, as well as the methods of constructing such theories, have received considerable attention for over fifty years. More recently, due to the development of new types of materials being considered for use in submersible and space-type structures, it has become desirable to include anisotropic material properties in the theory.

The current investigation will be devoted primarily to the problem of structural behavior of an elastic orthotropic shallow arch including transverse shear and transverse normal stress effects and undergoing finite deflections. The effect of initial imperfections is also considered in order to investigate possible bifurcation of the arch.

The general theory derived here, which considers transverse shear and transverse normal stress existing in an orthotropic arch is later specialized to the case of an isotropic arch with a consideration of shear deformation and is further specialized to the still simpler theory of the classical arch which is then compared to a theory derived independently. For the case of asymmetric deformation the transition from the initial state to the buckled state is shown to be connected with geometrical imperfections present in the structures.

A survey of the literature on arches reveals that many papers have been published pertinent to the classical theory of arches. A general discussion and significant references up to 1955 covering buckling problems of circular rings and arches is given by S. Timoshenko and J. M. Gere [1]. These authors

show that in the case of very flat arches, buckling in which axial strain is considered may occur at a smaller load than inextensional buckling. Timoshenko assumed that the center line of the deflected arch as well as the initial no-load shape is a half wave of the sine curve and arrived at a very simple solution. A very complete investigation of structural behavior of a shallow arch is attributed to Y. C. Fung and A. Kaplan [2]. These authors presented a series solution for the case of an arch having a sinusoidal configuration at no-load. They also found that instability may be associated with a bifurcation into an asymmetric buckling mode. The same approach was employed earlier by C. Biezeno [3] but for the case of a circular arch loaded by a concentrated normal force at the center. K. Federhofer solved the buckling problem of a parabolic arch in 1934 [4] and discussed the dynamic problems of arches and rings later [5]. K. O. Friedrichs [6] and K. Marguerre [7] derived the equations for a circular arch under uniformly distributed pressure by variational principles. K. O. Friedrichs pointed out that the uniform load corresponding to unsymmetric buckling could be much lower than that for symmetric buckling and in addition advanced a criterion for the buckling load as "the lowest load at which a buckled state exists having the same energy level as the unbuckled state at the same load." The so-called equal-energy criterion due to A. Gjelsvick and S. R. Bodner [8], although not generally accepted as a proper buckling criterion may lead to an "energy load" that represents a significant lower bound to the buckling load. H. Schreyer and E. Masur [9] gave the solution for the structural behavior of a clamped circular, shallow arch together with a detailed analysis of the various buckling criteria by considering the buckling equations and using the change in potential energy between the buckled and unbuckled states.

Notable contributions to the theories of higher orders of accuracy which include the effects of either or both transverse normal stress and shear deformation are due to F. Hildebrand, E. Reissner and G. Thomas [10], A. E.

Green and W. Zerna [11], E. Reissner [12], and by P. M. Naghdi [13]. In reference [10], orthotropic shells are considered and the various theories which are derived from different approximations in the assumptions are compared and discussed. A. E. Green and W. Zerna concluded that the inclusion of shearing forces is likely to be of importance mainly in the case of edge effects. E. Reissner's work on obtaining stress-strain relations by removing the first approximation of Love [14] results in some simplifications as compared with those given in [10] and [11]. Later P. M. Naghdi included, in addition to the transverse shear and transverse normal stress, the rotatory inertia in isotropic shell analysis. E. Reissner [15] in a separate work discussed a problem concerning the torsion of a rectangular plate and this work has become the standard of comparison in the linear bending theory of elastic flat plates which includes transverse shear effects. In the large deformation range, P. Wilson [16] investigated the elastic circular flat plate with the transverse shear effect taken into account and R. R. Archer [17] derived a nonlinear shear deformation theory for isotropic shells. In the present investigation, the initial imperfections are also introduced to achieve better correspondence with the true structure. This leads to lower buckling loads.

# CHAPTER II

# CLASSICAL THEORY

## II.1. Introduction

In this chapter the classical theory will be developed and the critical loads corresponding to various values of the arch parameters, $\lambda$ , will be determined. The von Kármán type nonlinear strain-displacement relations are used. The arch considered here is circular, thin and shallow. In order to obtain a theory for the arch which is similar to the Euler-Bernoulli beam theorem, we make the following assumptions:*

(a) A normal to the undeformed arch middle surface is deformed without change of length into a normal to the deformed middle surface. The change in direction of the normal to the middle surface is neglected. Thus the change in direction of the transverse load is then neglected.

(b) The stress in direction of the normal to the middle surface is small compared to the other stresses.

(c) The ratio of thickness h to the radius of curvature R, is negligibly small compared to unity.

(d) The magnitude of transverse deflection is of the same order as the thickness of the arch.

(e) The load is considered to be applied at the middle surface.

The theory is called classical in the sense that it is based on these assumptions which result in ignoring the effects of shear and the transverse normal stress.

Based on these assumptions, the governing differential equations are derived by the principle of minimum potential energy. A finite difference

---

* This assumption is similar to the Kirchhoff assumption of plate theory or Love's first approximation of shell theory.

scheme together with Newton's iteration technique is used to solve the equations. Initial imperfections are also considered.

## II.2. Strain-Displacement, Stress-Strain Relations

Let the origin of an x-z coordinate system be located at one end of the arch with x being the coordinate extending along the middle surface of the arch and z being the distance of an arbitrary point measured along the outward normal to the middle axis of the arch (see Fig. 1(a)). For strain-displacement relations, let us employ the von Kármán type approximation in which the only non-linear terms retained are those corresponding to quadratic effects in the transverse displacement and its derivatives. Thus the strain-displacement relation is

$$\varepsilon_x = U,_x + \frac{W}{R} + \frac{1}{2}\left[\frac{\partial W}{\partial x}\right]^2 - \frac{1}{2}\left(\frac{\partial W_o}{\partial x}\right)^2 - \frac{W_o}{R} \tag{2.1}$$

where U,W are the displacement components at an arbitrary point in the arch in the x,z directions respectively and $W_o$ is the initial imperfection in the radial direction (see [18]).

The Euler-Bernoulli type theorem as stated in section 2.1, leads to

$$\begin{aligned} U(x,z) &= u(x) - z[w(x) + w_o(x)],_x \\ W(x) &= w(x) + w_o(x) \end{aligned} \tag{2.2}$$

where u(x) and w(x) are the components of displacements at the middle surface.

By substituting (2.2) into (2.1), the strain-displacement relation becomes

$$\begin{aligned} \varepsilon_x &= u,_x + \frac{W}{R} + \frac{1}{2} w,_x^2 + w_{o,x}\, w,_x - z\,(w,_{xx} + w_{o,xx}) \\ &= \varepsilon_x^o + zK_x \end{aligned} \tag{2.3}$$

where $\varepsilon_x^o = u,_x + \frac{W}{R} + \frac{1}{2}w,_x^2 + w_{o,x}w,_x$ and $K_x = -w,_{xx} - w_{o,xx}$ are the middle surface strain and the change of curvature, respectively.

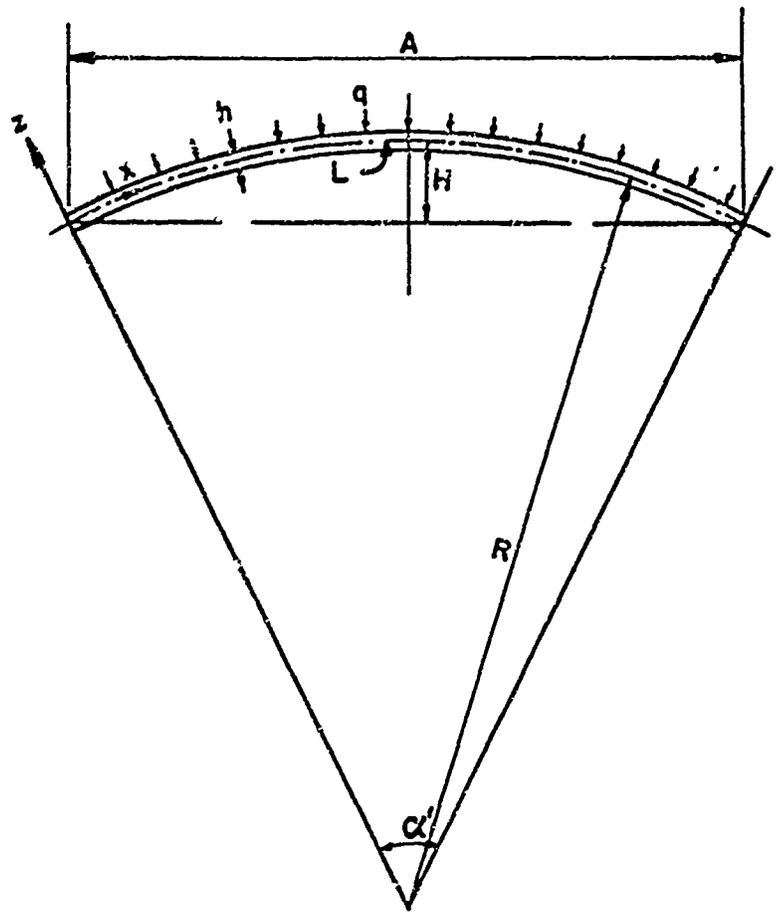


(a) COORDINATE SYSTEM & GEOMETRY

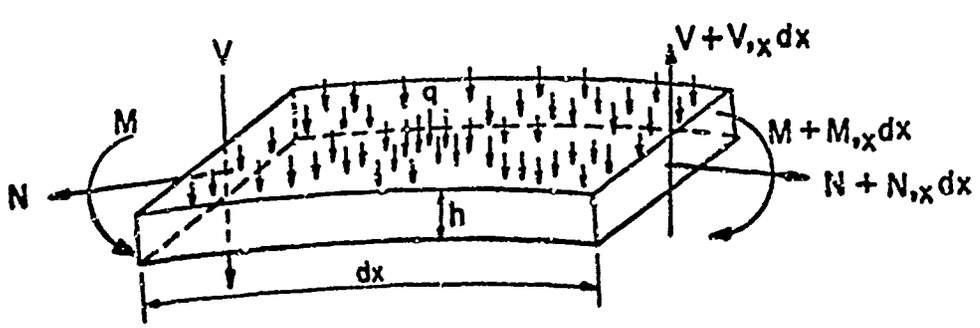


(b) ARCH ELEMENT

FIG. 1 THE CONFIGURATION OF THE ARCH

The stress-strain relationship, assuming Hooke's law holds, is

$$\sigma_x = E\varepsilon_x \tag{2.4}$$

or conversely

$$\varepsilon_x = \frac{\sigma_x}{E}. \tag{2.5}$$

II.3. Derivation of Equilibrium Equations and Natural Boundary Conditions

The strain energy density $U_0$ is a function of the strain component [19], i.e.:

$$U_0 = U_0(\varepsilon_x) \tag{2.6}$$

If the displacement vector $(u,w)$ receives variations $(\delta u, \delta w)$, the strain tensor assumes a variation $\delta\varepsilon_x$ and the corresponding variation of $U_0$ is

$$\delta U_0 = \frac{\partial U_0}{\partial \varepsilon_x}\,\delta\varepsilon_x.$$

It has been shown that the following relation holds for a Hookean material in the large deformation range [19],

$$\sigma_x = \frac{\partial U_0}{\partial \varepsilon_x}$$

Therefore

$$\delta U_0 = \sigma_x \delta\varepsilon_x \tag{2.7}$$

Substituting (2.3) into (2.7), one finds

$$\delta U_0 = \sigma_x(\delta\varepsilon_x^0 + z\delta K_x).$$

Let the first variation of the strain energy of the entire arch be $\delta U_T$. Then

$$\delta U_T = \int_0^L \int_{-\frac{h}{2}}^{\frac{h}{2}} \delta U_0 \, dz dx$$

$$= \int_0^L \int_{-\frac{h}{2}}^{\frac{h}{2}} \sigma_x(\delta\varepsilon_x^0 + z\delta K_x) dz dx \tag{2.8}$$

or

$$\delta U_T = \int_0^L \int_{-\frac{h}{2}}^{\frac{h}{2}} E[\varepsilon_x^o \, \delta\varepsilon_x^o + z(\varepsilon_x^o \, \delta K_x + K_x \, \delta\varepsilon_x^o) + z^2 K_x \, \delta K_x] dz dx$$

Upon integration with respect to z, one finds

$$\delta U_T = \int_0^L (Eh \, \varepsilon_x^o \, \delta\varepsilon_x^o + \frac{Eh^3}{12} K_x \, \delta K_x) dx \tag{2.9}$$

$$= \delta U_m + \delta U_b$$

where $\delta U_m = \int_0^L Eh \, \varepsilon_x^o \, \delta\varepsilon_x^o \, dx$ is the membrane strain energy and

$\delta U_b = \int_0^L \frac{Eh^3}{12} K_x \, \delta K_x \, dx$ is the bending strain energy.

The force and moment resultants, N and M (per unit width of arch) shown in Fig. 1(b) take the form

$$N = \int_{-\frac{h}{2}}^{\frac{h}{2}} \sigma_x dz \tag{2.10}$$

$$M = \int_{-\frac{h}{2}}^{\frac{h}{2}} z\sigma_x dz, \tag{2.11}$$

which upon integration with respect to z become

$$\begin{aligned} N &= Eh(u_{,x} + \frac{w}{R} + w_{o,x} \, w_{,x} + \frac{1}{2} w_{,x}^2) = Eh \, \varepsilon_x^o \\ M &= -\frac{Eh^3}{12}(w_o + w)_{,xx} = \frac{Eh^3}{12} K_x \end{aligned} \tag{2.12}$$

Substituting these force and moment resultants into the first variation of the total strain energy (2.9), we get

$$\delta U_T = \int_0^L [N \, \delta\varepsilon_x^o + M \, \delta K_x] \, dx \tag{2.13}$$

Now, substituting (2.3) into (2.13), we get

$$\delta U_T = \int_0^L \{N[\delta(u,_x) + \frac{1}{R}\,\delta w + w_{o,x}\,\delta(w,_x) + w,_x\,\delta(w,_x)]$$

$$-M[\delta(w,_{xx})]\}\,dx \tag{2.14}$$

The potential energy due to the external load q is

$$\Omega = -\int_0^L q(w + w_o)\,dx$$

and the total potential energy $\Pi$ is then

$$\Pi = U_T + \Omega.$$

By variation of $\Pi$, we get the equilibrium equations and the associated natural boundary conditions. The equilibrium equations are:

$$N,_x = 0 \tag{2.16}$$

$$N(\frac{1}{R} - w,_{xx} - w_{o,xx}) - M,_{xx} - q = 0$$

and the natural boundary conditions are:

$N = 0$ or u prescribed at $x = 0$ and L

$Nw,_x + M,_x = 0$ or w prescribed at $x = 0$ and L*

$M = 0$ or $w,_x$ prescribed at $x = 0$ and L

Substituting (2.12) into (2.16), we get

$$U,_{xx} + \frac{1}{R}\,w,_x + w_{o,x}\,w,_{xx} + w_{o,xx}\,w,_x + w,_x\,w,_{xx} = 0$$

$$\frac{Eh^3}{12}(w_o + w),_{xxxx} + Eh\,(U,_x + \frac{w}{R} + w_{o,x}\,w,_x + \frac{1}{2}\,w,_x^2)$$

$$\cdot(\frac{1}{R} - w_{o,xx} - w,_{xx}) - q = 0 \tag{2.17}$$

II.4. Solution to the Equations

Let us introduce the following nondimensional variables

---

* $Nw,_x + M,_x$ corresponds to shear forces V in Fig. 1(b).

$$x = Ls$$
$$u = \frac{h^2}{L}\phi$$
$$w = h\alpha$$
$$\bar{w}_0 = \frac{w_0}{h}$$
and $$\lambda = \frac{L^2}{Rh},$$

The equations (2.17) then take the form:

$$\phi_{,ss} + \lambda\alpha_{,s} + \bar{w}_{0,s}\,\alpha_{,ss} + \bar{w}_{0,ss}\,\alpha_{,s} + \alpha_{,s}\,\alpha_{,ss} = 0 \tag{2.18a}$$

$$\frac{1}{12}(\alpha + \bar{w}_0)_{,ssss} + (\lambda - \bar{w}_{0,ss} - \alpha_{,ss})\left(\phi_{,s} + \lambda\alpha + \bar{w}_{0,s}\,\alpha_{,s} + \frac{1}{2}\alpha_{,s}^2\right) - Q = 0^* \tag{2.18b}$$

where $Q = qL^4/Eh^4$

Let us next linearize these equations in order to obtain a system that can be treated by Newton's iteration scheme [20]. Regarding the displacement components $\phi$ and $\alpha$ and their derivatives as independent variables, let us expand the nonlinear terms of those variables into Taylor series using as a starting point the no-load equilibrium configuration and retaining only the nonlinear parts. Typical expansions of the terms are as follows:

$$\alpha_{,s}\,\alpha_{,ss} = \bar{\bar{\alpha}}_{,s}\,\bar{\bar{\alpha}}_{,ss} + \bar{\bar{\alpha}}_{,s}(\alpha_{,ss} - \bar{\bar{\alpha}}_{,ss}) + \bar{\bar{\alpha}}_{,ss}(\alpha_{,s} - \bar{\bar{\alpha}}_{,s})$$
$$= \bar{\bar{\alpha}}_{,s}\,\alpha_{,ss} + \bar{\bar{\alpha}}_{,ss}\,\alpha_{,s} - \bar{\bar{\alpha}}_{,s}\,\bar{\bar{\alpha}}_{,ss}$$
$$\alpha_{,ss}\,\alpha_{,s}^2 = 2\bar{\bar{\alpha}}_{,ss}\,\bar{\bar{\alpha}}_{,s}\,\alpha_{,s} + \bar{\bar{\alpha}}_{,s}^2\,\alpha_{,ss} - 2\bar{\bar{\alpha}}_{,ss}\,\bar{\bar{\alpha}}_{,s}^2$$

where the double barred quantities are the estimates of the same unbarred quantities. The linearized versions of the equations (2.18) are

$$\phi_{,ss} + \lambda\alpha_{,s} + \bar{w}_{0,s}\,\alpha_{,ss} + \bar{w}_{0,ss}\,\alpha_{,s} + \bar{\bar{\alpha}}_{,ss}\,\alpha_{,s} + \bar{\bar{\alpha}}_{,s}\,\alpha_{,ss} = \bar{\bar{\alpha}}_{,s}\,\bar{\bar{\alpha}}_{,ss} \tag{2.19a}$$

$$\frac{1}{12}\alpha_{,ssss} + (\lambda - \alpha_{,ss} - \bar{w}_{0,ss})\left(\phi_{,s} + \lambda\alpha + \bar{w}_{0,s}\,\alpha_{,s} + \bar{\bar{\alpha}}_{,s}\,\alpha_{,s}\right)$$

---

* In [6], because of (2.16), $(\varphi_{,s} + \lambda\alpha\,\bar{w}_{0,s}\,\alpha_{,s} + \frac{1}{2}\alpha_{,s}^2)$ was treated as constant.

$$-(\bar{\bar{\phi}}_{,s} + \lambda\bar{\bar{\alpha}} + \frac{1}{2}\bar{\bar{\alpha}}_{,s}^{2})\,\alpha_{,ss} = -\frac{1}{12}W_{o,ssss} + \frac{1}{2}\lambda\bar{\bar{\alpha}}_{,s}^{2} - \bar{\bar{\phi}}_{,s}\,\bar{\bar{\alpha}}_{,ss}$$

$$- \lambda\bar{\bar{\alpha}}\,\bar{\bar{\alpha}}_{,ss} - \bar{\bar{\alpha}}_{,ss}\,\bar{\bar{\alpha}}_{,s}^{2} - \frac{1}{2}\bar{W}_{o,ss}\,\bar{\bar{\alpha}}_{,s}^{2} - \bar{W}_{o,s}\,\bar{\bar{\alpha}}_{,s}\,\bar{\bar{\alpha}}_{,ss} + Q \tag{2.19b}$$

The quantities without bars in (2.19) are approximated by central differences. If we select $\tilde{N}$ internal grid points in the x direction, the grid increment is then $1/\tilde{N}+1$ and equation (2.19) becomes

$$D^2\,\delta_s^2\,\phi_i + \frac{D}{2}\lambda\delta_s\alpha_i + D^2\,\bar{W}_{o,s}\,\delta_s^2\,\alpha_i + \frac{D}{2}\bar{W}_{o,ss}\,\delta_s\,\alpha_i + \frac{D}{2}\bar{\bar{\alpha}}_{,ss}\,\delta_s\,\alpha_i$$

$$+ D^2\,\bar{\bar{\alpha}}_{,s}\,\delta_s^2\,\alpha_i = \bar{\bar{\alpha}}_{,s}\,\bar{\bar{\alpha}}_{,ss} \tag{2.20a}$$

$$\frac{D^4}{12}\delta_s^4\,\alpha_i + (\lambda - \bar{W}_{o,ss} - \bar{\bar{\alpha}}_{,ss})\,(\frac{D}{2}\delta_s\,\phi_i + \lambda\alpha_i + \frac{D}{2}\bar{W}_{o,s}\,\delta_s\,\alpha_i + \frac{D}{2}\bar{\bar{\alpha}}_{,s}\,\delta_s\,\alpha_i)$$

$$-(\bar{\bar{\phi}}_{,s} + \lambda\bar{\bar{\alpha}} + \frac{1}{2}\bar{\bar{\alpha}}_{,s}^{2})\,D^2\,\delta_s^2\,\alpha_i = -\frac{1}{12}\bar{W}_{o,ssss} + \frac{1}{2}\lambda\bar{\bar{\alpha}}_{,s}^{2} - \bar{\bar{\phi}}_{,s}\,\bar{\bar{\alpha}}_{,ss}$$

$$- \lambda\bar{\bar{\alpha}}\,\bar{\bar{\alpha}}_{,ss} - \bar{\bar{\alpha}}_{,ss}\,\bar{\bar{\alpha}}_{,s}^{2} - \frac{1}{2}\bar{W}_{o,ss}\,\bar{\bar{\alpha}}_{,s}^{2} - \bar{W}_{o,s}\,\bar{\bar{\alpha}}_{,s}\,\bar{\bar{\alpha}}_{,ss} + Q \tag{2.20b}$$

where $D = \tilde{N} + 1$

$$\delta_s\,\phi_i = \phi_{i+1} - \phi_{i-1}$$

$$\delta_s^2\,\phi_i = \phi_{i+1} - 2\phi_i + \phi_{i-1}$$

$$\delta_s^4\,\phi_i = \phi_{i+2} - 4\phi_{i+1} + 6\phi_i - 4\phi_{i-1} + \phi_{i-2}.$$

Equation (2.20) represents a system of $2\tilde{N}$ simultaneous nonlinear algebraic equations which are solved by Newton's iteration scheme using a digital computer. Ordinarily this has been done by input load increments as the known quantity to solve for $\phi$ and $\alpha$. However the procedure fails to give any information on the load-deflection relations after the first peak load is reached, since the slope is zero at this point and the computer yields unstable solutions. For the present case involving a consideration of imperfections, the extension of the load-deflection curve past its peak becomes desirable to be able to obtain the lower buckling load.

If deflection instead of load is employed as the input and load regarded as the unknown quantity, the above-mentioned difficulty is avoided and the load-deflection curve can be extended. But since the buckled mode shape of the arch is yet to be determined, the input of deflections is not realistic. As an alternate approach the summation of all radial displacements, i.e., the change of area between the arch and its base line can be employed by introducing an additional equation relating the area to the radial deflections, namely:

$$\text{AREA} = \frac{1}{\tilde{N}+1} \sum_{i=1}^{\tilde{N}} \alpha_i$$

This equation together with the previous $2\tilde{N}$ equations forms a system which has the right number of equations after the additional unknown Q is added.

Let us write the system in matrix form

$$[A]\,[X] = [B]$$

where [A] is a coefficient matrix, [B] is a constant column matrix and [X] the unknown column matrix. The loading term Q in (2.20b)is moved to the left hand side of the equation and is included in the unknown matrix [X]. The double barred quantities in [A] and [B] are assumed to be zero at the beginning of the iteration or more precisely, the displacement components are assumed to be zero at the beginning of the iteration. Then the independent area parameter AREA in [B] is given successive increments and the displacements determined. If the calculation for displacements converges, a further increment is employed.

If we neglect the imperfection terms in the equations, the solution for radial displacement $\alpha$ in general is symmetric with respect to the midpoint of the arch, since the equations are expressed in central differences and the boundary conditions are symmetric. However the symmetric characteristics of the system are of course disturbed if we impose an antisymmetric mode

of initial no-load imperfection. The resulting solution is then an asymmetric one and instability occurs at a lower load than in the case of symmetric buckling of an initially perfect arch.

For the hinged end arch, an antisymmetric sine curve is assumed to represent the no-load configuration, viz:

$$\bar{w}_0 = \bar{w}_{00} \sin 2\pi s$$

where $\bar{w}_{00}$ is the amplitude and a numerical value of 0.04 is used for numerical analysis. For the clamped end arch a polynomial corresponding to clamped end conditions and antisymmetric with respect to the mid-point of arch is used. The polynomial is $w_0 = w_{00}\,[As^6 + Bs^5 + Cs^4 + Ds^3 + Es^2]$, where $A = 2.048910 \times 10^{-8}$, $B = -1.137778 \times 10^2$, $C = 2.844444 \times 10^2$, $D = -2.275556 \times 10^2$, $E = 5.688889 \times 10$ and $w_{00} = 0.04$.

## II.5. Discussion of Results

Typical load-deflection curves for hinged end and clamped end arches are shown in Figs. 2 and 3 respectively. There, the asymmertic solution is obtained by imposing antisymmetric initial imperfections while the symmetric solution is the one obtained by setting the amplitude $\bar{w}_{00}$ equal to zero. To determine the load-deflection relations shortly before point "C" of Fig. 2 has been reached, the imperfection $w_{00}$ (introduced to force the asymmetric form to appear) is taken to be zero and the return branch cb is found. The bifurcation point "b" where the returning curve meets the symmetric curve is about 25 percent lower than the point "a" in this case.

The variation of load-deflection relation with the geometric parameter $\lambda$ is shown in Figs. 4 and 5. Figs. 6 and 7 show how the critical load increases with $\lambda$. From these figures the following conclusions* can be drawn:

(1) For the hinged end arch:

(a) For $\lambda \leq 6$, no buckling occurs;

* Figures are approximate values.

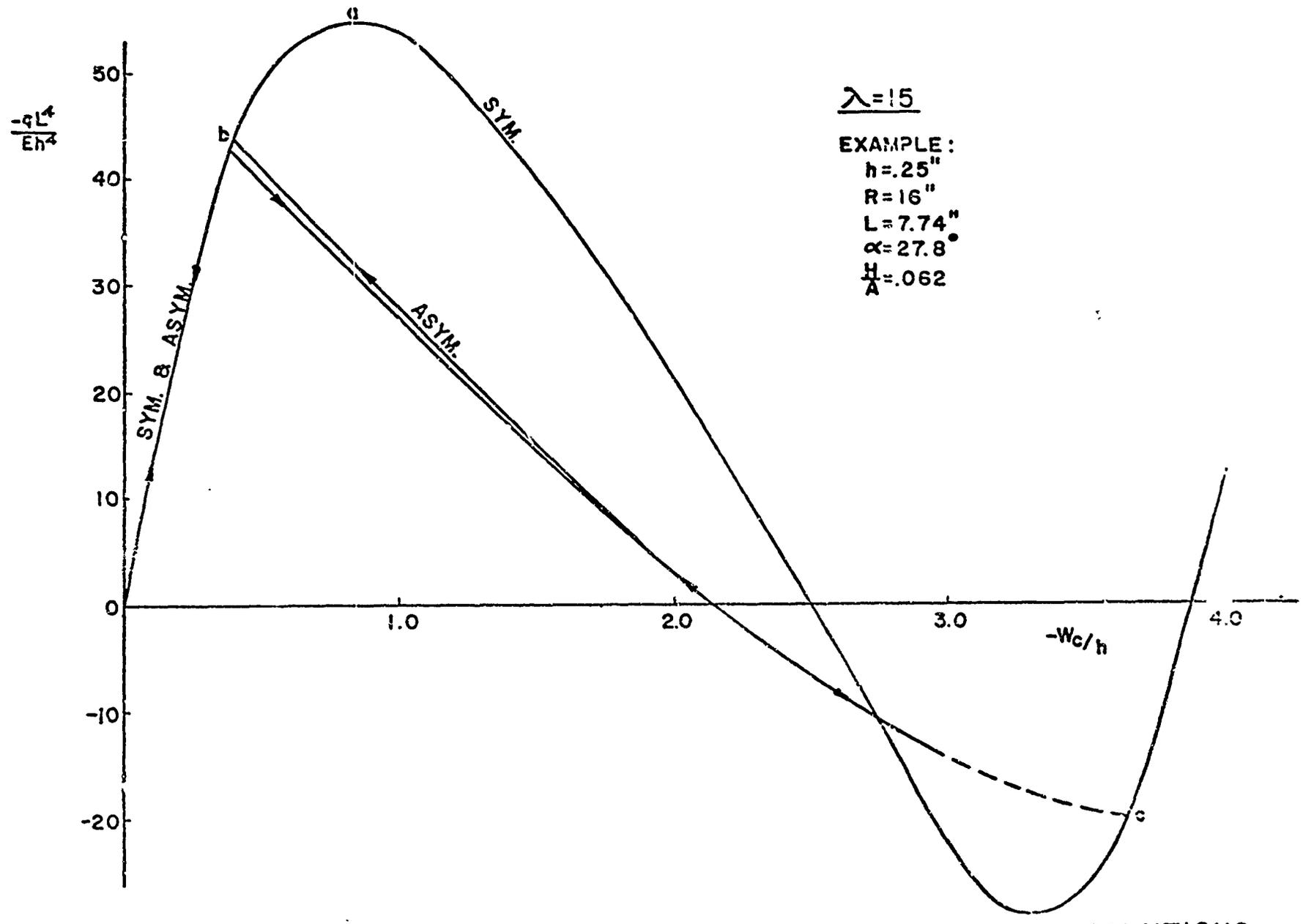


FIG. 2 LOAD-DEFLECTION CURVE FOR SYMMETRIC & ASYMMETRIC SOLUTIONS FOR HINGED ENDS

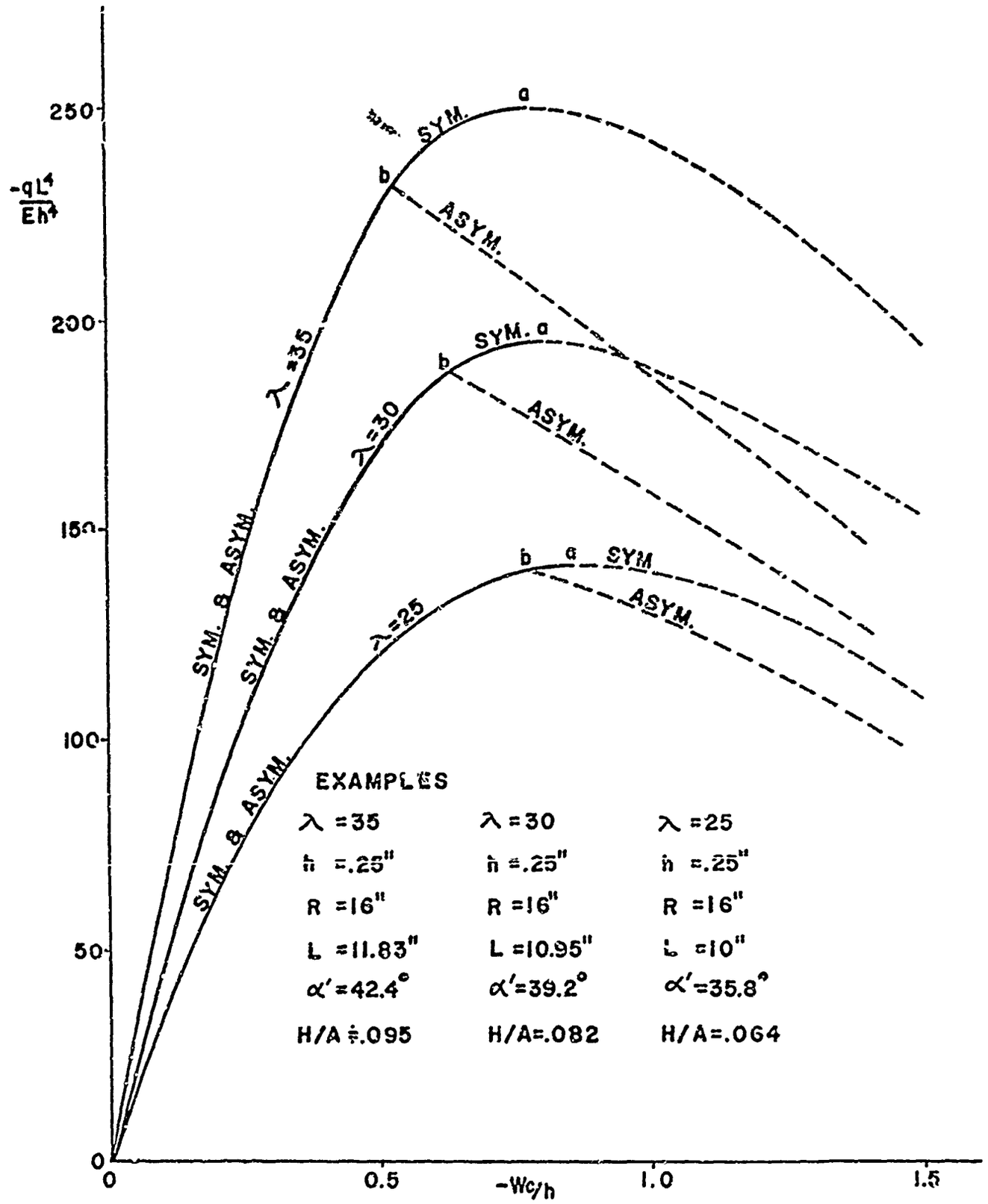


FIG.3 LOAD-DEFLECTION CURVES FOR CLAMPED ENDS

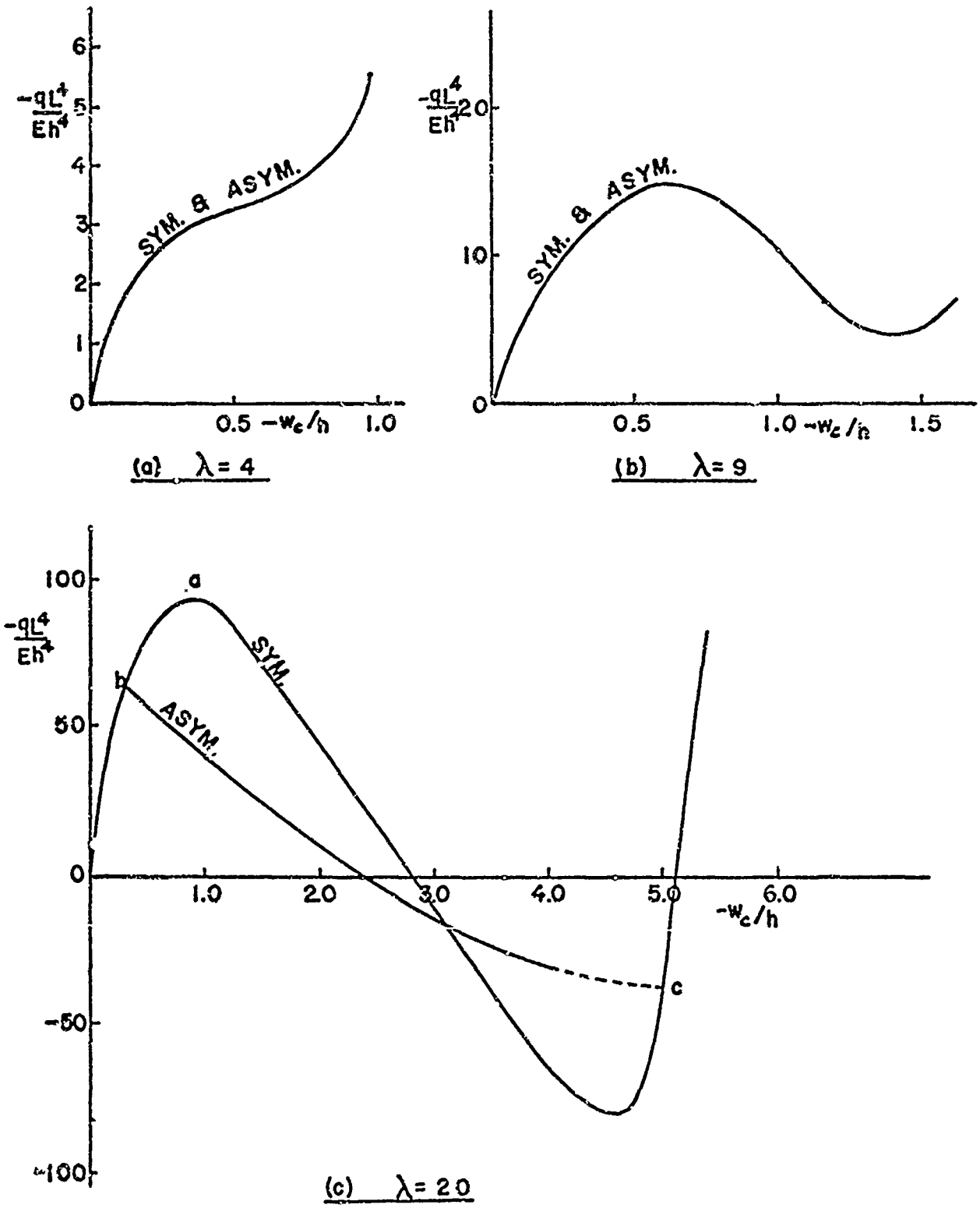


FIG. 4 LOAD-DEFLECTION CURVES FOR THE HINGED ENDS

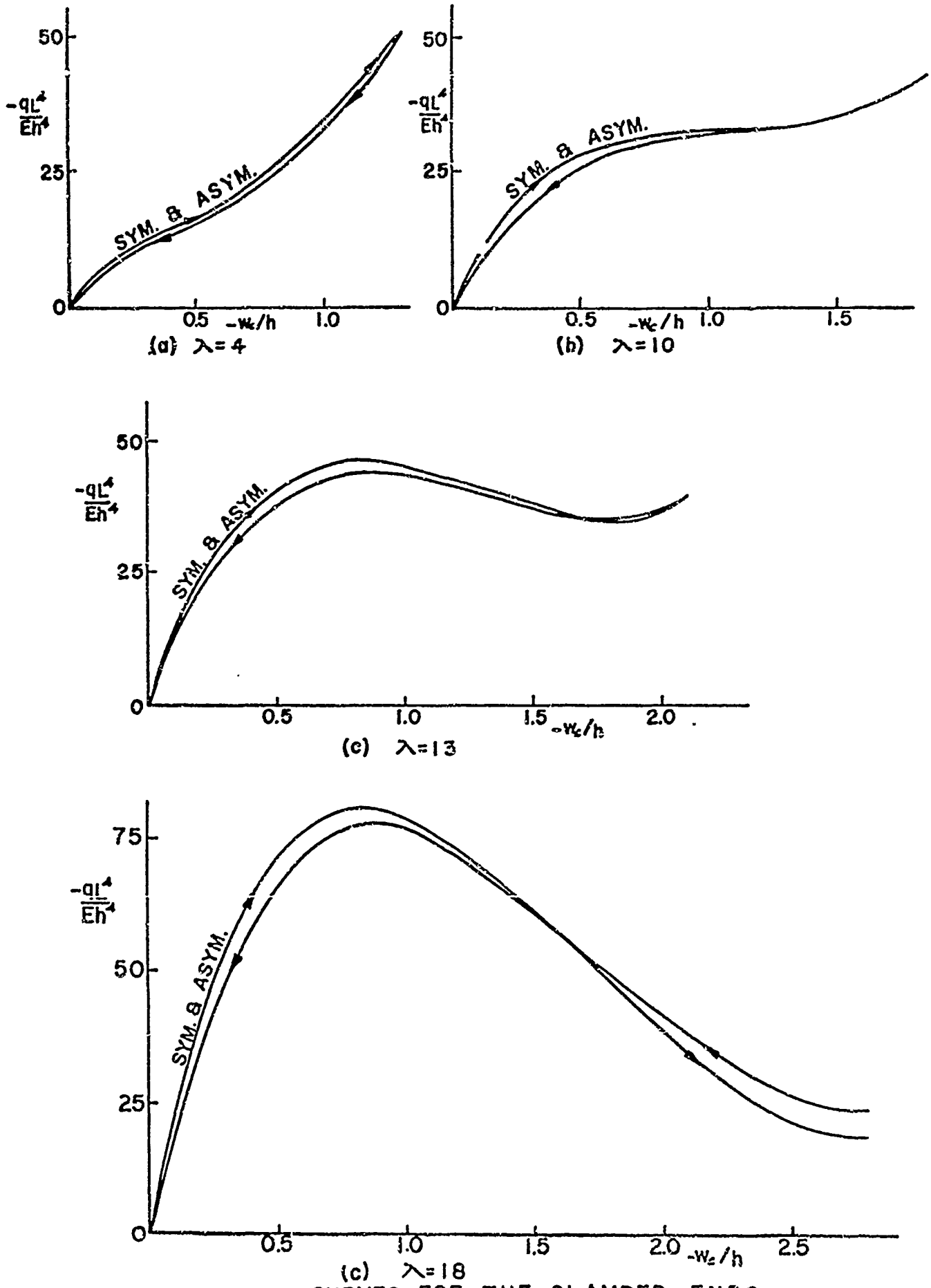


FIG. 5 LOAD-DEFLECTION CURVES FOR THE CLAMPED ENDS

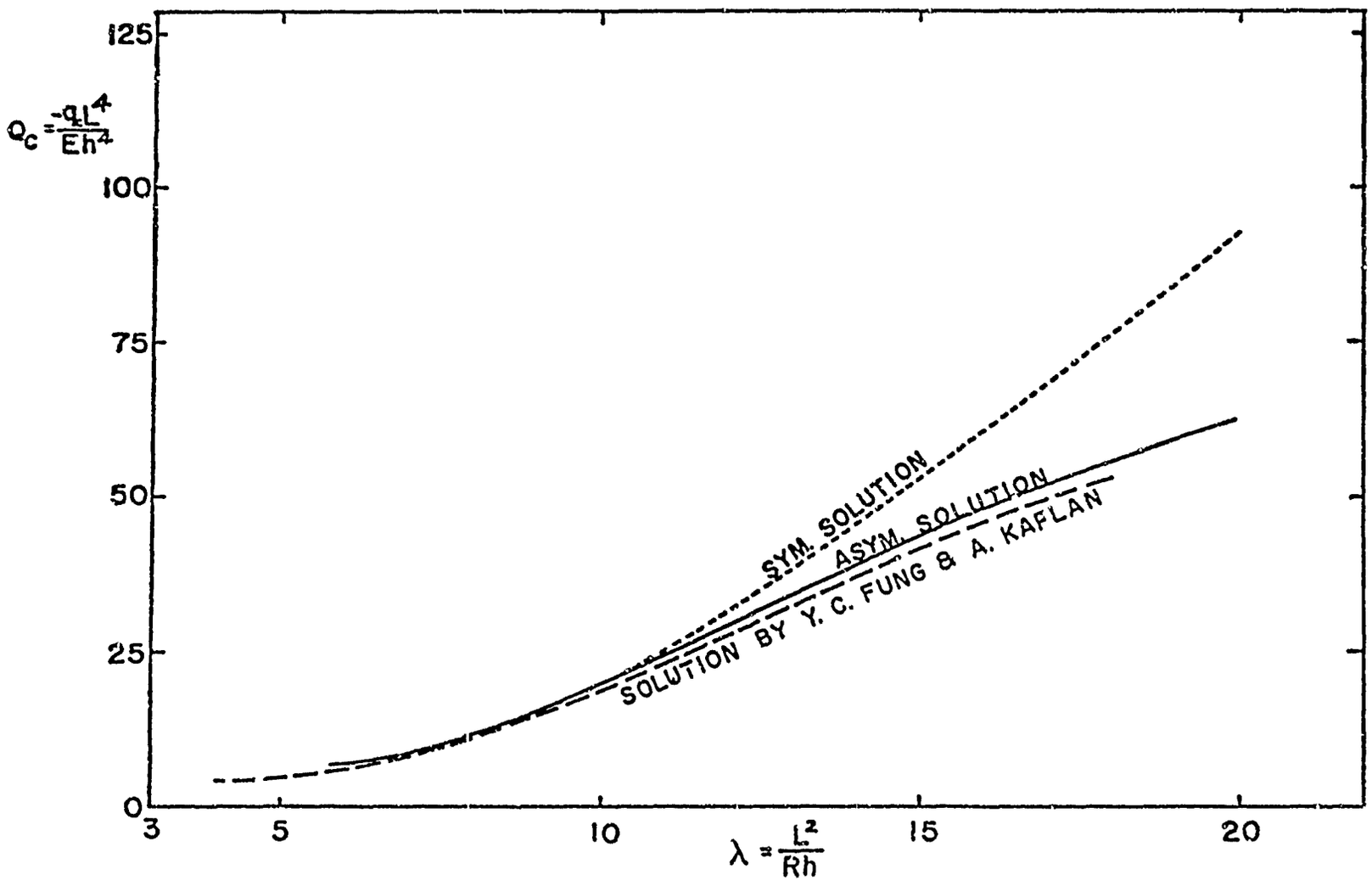


FIG. 6 $Q_c$-$\lambda$ CURVES FOR VARIOUS SOLUTIONS
HINGED ENDS

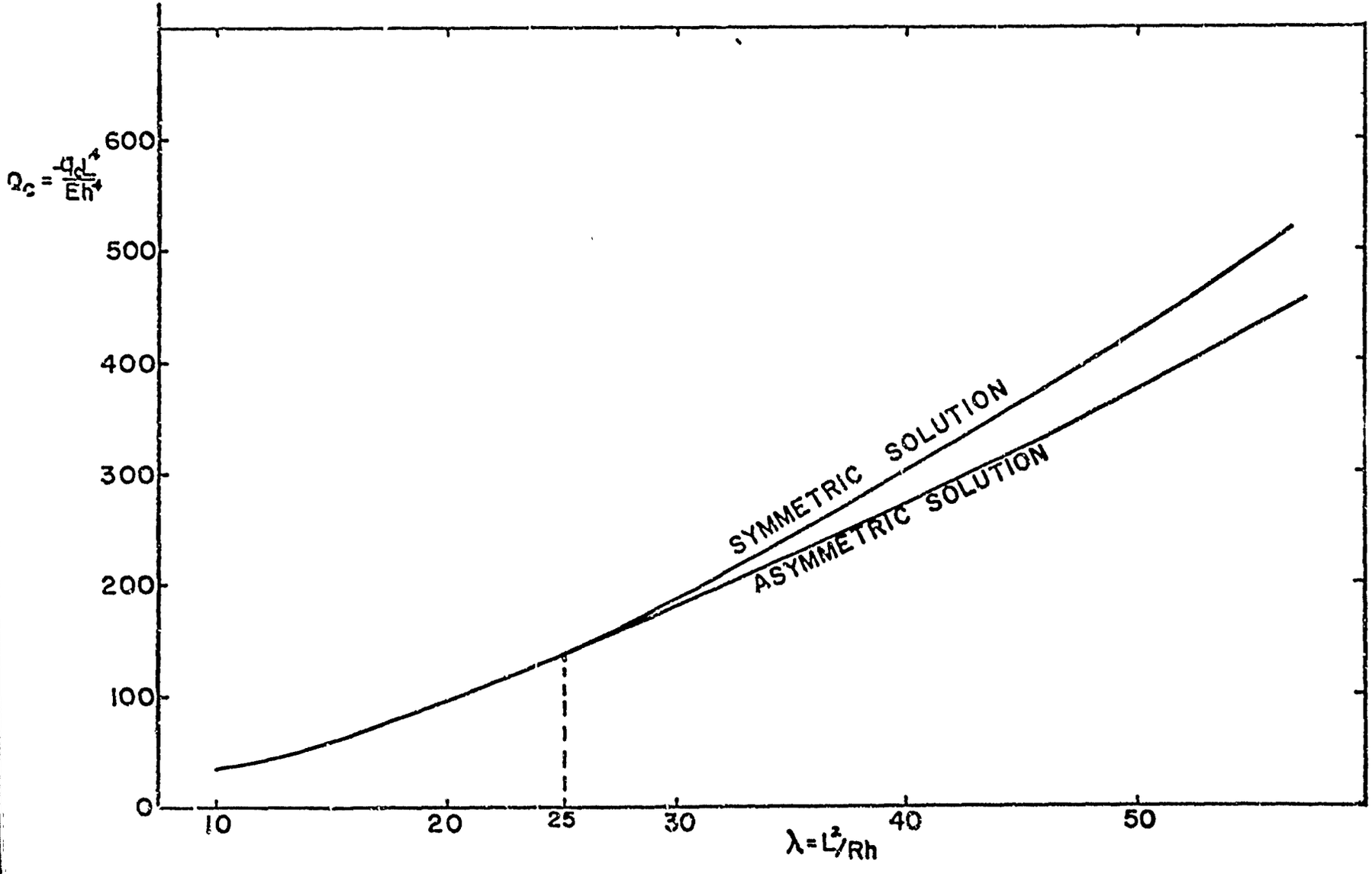


FIG. 7 $Q_c - \lambda$ CURVES FOR SYM. AND ASYM. SOLUTIONS
CLAMPED ENDS

(b) For $6 \leq \lambda \leq 10.8$ (10.5 by Y. C. Fung and A. Kaplan [2]), the buckling mode is symmetrical;

(c) For $\lambda \geq 10.8$, the asymmetric buckling criterion holds. The asymmetric solution found here agrees very closely with Y. C. Fung and A. Kaplan's solution [2] which is also plotted on Fig. 6.

(2) For the clamped end arch:

(a) For $\lambda \leq 10.0$ (11.4 by H. Schreyer and E. Masur [9]), no buckling occurs;

(b) For $10.0 \leq \lambda \leq 25$ (22.96 by H. Schreyer and E. Masur [9]), the arch behavior is governed by the symmetric criterion;

(c) For $\lambda \geq 25$, the asymmetric buckling criterion holds.

# CHAPTER III

# TRANSVERSE SHEAR DEFORMATION AND TRANSVERSE NORMAL STRESS THEORY TOGETHER WITH A CONSIDERATION OF INITIAL IMPERFECTIONS

## III.1. Introduction

The Euler-Bernoulli beam type theorem assumed in section II.1 which is similar to the Kirchhoff assumption of plate theory or Love's first approximation of shell theory results in neglecting the transverse shear deformation and transverse normal stress.

Due to recent developments of new types of material, the orthotropic feature of many materials must be taken into account. The present investigation is particularly concerned with materials in which the reinforcement consists of glass fibers embedded in an epoxy matrix with every glass fiber oriented toward the center of curvature of the structure, in this case an arch. This radial filament construction offers the advantage of the fiber being loaded in transverse compression rather than in axial compression which may lead to column-type instability. The resin is restrained from extrusion from between the glass fibers by shear coupling to the fibers, thereby placing the filaments under axial tension. Thus the inclusion of transverse normal stress and shear effects may be of importance. With inclusion of these effects, an Euler-Bernoulli beam type assumption is inadequate. And a modification to Euler-Bernoulli type assumption (c) lies in not completely neglecting the ratio z/R with respect to unity but instead writing $\frac{1}{1+z/R} \approx 1 - \frac{z}{R} + (\frac{z}{R})^2$ in the strain-displacement relations.

The initial radial imperfections of the middle surface are included in the derivation to more nearly agree with reality. This leads to a lower asymmetric buckling load. Reissner's Variational Theorem [21] is used to derive the equilibrium equations as well as the stress-strain relations.

The numerical method outlined in the foregoing chapter is used to solve the equations

III.2. Strain-Displacement Relations

Let us use the coordinate system described in section II.2. and also the von Kármán type non-linear strain-displacement relations. The transverse normal strain $\varepsilon_z$ and transverse shear strain $\gamma_{xz}$ together with $\varepsilon_x$ now describe the state of strain, viz:

$$\varepsilon_x = \frac{1}{1+\frac{z}{R}}\left(U_{,x} + \frac{W}{R}\right) + \frac{1}{(1+\frac{z}{R})^2}\left(\frac{1}{2} W_{,x}^2 + W_{,x} W_{o,x}\right)$$

$$\varepsilon_z = W_{,z} \tag{3.1}$$

$$\gamma_{xz} = \frac{1}{1+\frac{z}{R}} W + U_{,z} - \frac{1}{R(1+\frac{z}{R})} U$$

where $w_o$ is the initial imperfection in the radial direction (see [18]). Let us introduce the displacement approximations

$$U(x,z) = u(x) + zu'(z) \tag{3.2a}$$

$$W(x,z) = w(x) + zw'(x) + \frac{1}{2} z^2 w''(x) \tag{3.2b}$$

Substituting (3.2) into (3.1) and multiplying (3.1a) and (3.1c) by $(1+\frac{z}{R})$, we get

$$(1+\frac{z}{R})\,\varepsilon_x = \varepsilon_x^o + zK_x + \frac{z^2}{2} K_x' + \frac{z^3}{3!} K_x'' + \frac{z^4}{4!} K_x''' + \frac{z^5}{5!} K_x^{iv} + \frac{z^6}{6!} K_x^{v}$$

$$\varepsilon_z = \varepsilon_z^o + zK_z \tag{3.3}$$

$$(1+\frac{z}{R})\,\gamma_{xz} = \gamma_{xz}^o + zK_{xz} + \frac{z^2}{2} K_{xz}'$$

where

$$\varepsilon_x^o = u_{,x} + \frac{1}{R} w + \frac{1}{2} w_{,x}^2 + w_{,x} w_{o,x} \tag{3.3d}$$

$$K_x = u_{,x}' + \frac{1}{R} w' - \frac{C_1}{2R} w_{,x}^2 + w_{,x} w_{,x}' + w_{,x}' w_{o,x} - \frac{C_1}{R} w_{,x} w_{o,x} \tag{3.3e}$$

$$K_x' = \frac{1}{R} w'' + w_{,x}'^2 + w_{,x} w_{,x}'' - \frac{2C_1}{R} w_{,x} w_{,x}' + \frac{C_1}{R^2} w_{,x}^2 + \frac{2C_1}{R^2} w_{,x} w_{o,x}$$
$$- \frac{2C_1}{R} w_{o,x} w_{,x}' + w_{o,x} w_{,x}'' \tag{3.3f}$$

$$K_x'' = 6\cdot\left(\frac{1}{2} w_{,x}' w_{,x}'' - \frac{C_1}{2R} w_{,x}'^2 - \frac{1}{2R} w_{,x} w_{,x}'' + \frac{C_1}{R^2} w_{,x} w_{,x}' + \frac{C_1}{R^2} w_{o,x} w_{,x}'\right.$$
$$\left. - \frac{C_1}{2R} w_{o,x} w_{,x}''\right) \tag{3.3g}$$

$$K_x''' = 24\cdot\left(\frac{1}{8} w_{,x}''^2 - \frac{C_1}{2} w_{,x}' w_{,x}'' + \frac{C_1}{2R^2} w_{,x}'^2 + \frac{C_1}{2R^2} w_{,x} w_{,x}'' + \frac{C_1}{2R^2} w_{o,x} w_{,x}''\right) \tag{3.3h}$$

$$K_x^{iv} = 120\cdot\left(- \frac{C_1}{8R} w_{,x}'' + \frac{C_1}{2R^2} w_{,x}' w_{,x}''\right) \tag{3.3i}$$

$$K_x^{v} = 720\cdot\left(\frac{C_1}{8R^2} w_{,x}''^2\right) \tag{3.3j}$$

$$\varepsilon_z^o = w' \tag{3.3k}$$

$$K_z = w'' \tag{3.3l}$$

$$\gamma_{xz}^o = - \frac{u}{R} + u' + w_{,x} \tag{3.3m}$$

$$K_{xz} = w_{,x}' \tag{3.3n}$$

and $$K_{xz}' = w_{,x}''. \tag{3.3o}$$

The coefficient $C_1$ is introduced to distinguish the modification in this theory from the Euler-Bernoulli type theorem.

## III.3. Derivation of Stress Strain Relations and Equilibrium Equations

If the force resultant N, the moment M and the transverse shear resultant V (all per unit length of middle surface) are defined in the conventional manner, viz:

$$N = \int_{-\frac{h}{2}}^{\frac{h}{2}} \sigma_x \, dz \ , \quad V = \int_{-\frac{h}{2}}^{\frac{h}{2}} \tau_{xz} \, dz \ , \ M = \int_{-\frac{h}{2}}^{\frac{h}{2}} \sigma_x \, zdz. \tag{3.4}$$

then we assume that (see [13])

$$\sigma_x = \frac{N}{h} + \frac{M}{h^2/6}\frac{z}{h/2} = \frac{N}{h} + \frac{12M}{h^3} z \tag{3.5}$$

$$\tau_{xz} = \frac{3}{2}\frac{V}{h}[1 - (\frac{z}{h/2})^2] = \frac{3V}{2h}[1 - \frac{4z^2}{h^2}] \tag{3.6}$$

$$(1+\frac{z}{R})\ \sigma_z = C_2\ \{[\frac{3}{2}\frac{S}{h} + \frac{T}{4h}(\frac{z}{h/2})][1 - (\frac{z}{h/2})2] + \frac{1}{2}\ qH[1+\frac{3}{2}(\frac{z}{h/2}) - \frac{1}{2}(\frac{z}{h/2})^3]\} \tag{3.7}$$

Here the functions S and T are as yet undetermined; q is the value of the load applied at the top surface of the arch,

$$H = 1 + \frac{h}{2}(\frac{1}{R})$$

and $C_2$ is introduced for the purpose of distinguishing between the contributions of transverse shear deformation and normal stress, ($C_2 = 0$), otherwise, it should be regarded as unity.

A convenient derivation of appropriate stress-strain relations, equilibrium equations and natural boundary conditions can be carried out by means of a variational theorem due to Reissner [21], viz:

$$\begin{aligned}\delta\ \{\iiint\ [\ \sigma_x\ \varepsilon_x + \tau_{xy}\ \gamma_{xy} + \sigma_z\ \varepsilon_z - A]\ (1+\frac{C_1 z}{R})\ dx\ dy\ dz \\ - \iint\ q(w + \frac{h}{2}w' + \frac{h^2}{8}\ w'')\ (1+\frac{C_1 h}{2R})\ dx\ dy\} = 0\end{aligned} \tag{3.8}$$

where for an orthotropic material

$$A = \frac{1}{2E_x}\ [\sigma_x^2 + \frac{\nu_{xz}}{\nu_{zx}}\sigma_z^2 + \frac{E_x}{G}\tau_{xz}^2 - 2\nu_{xz}\ \sigma_x\ \sigma_z]. \tag{3.9}$$

Integrating (3.8) with respect to z, carrying out the variations and integrating by parts, the stress-strain relations, the equilibrium equations and associated boundary conditions are obtained.

The coefficients of $\delta w'$ and $\delta w''$ give the expressions for S and T respectively. A simplification is made by neglecting the nonlinear terms and also the shear term V, since as the arch becomes thinner the effects of S and

T, i.e. the effects of transverse normal stress, becomes negligible. Thus the equation (3.5) in reference [13] is used:

$$S = -\frac{M}{R} \tag{3.10}$$

$$T = -\frac{5h}{2R} N + \frac{3hH}{2} q \tag{3.11}$$

The coefficients of $\delta N$ and $\delta M$ give the relations for M, N and displacement components. They are

$$N = E_x h\,(AA)\,[1 - \frac{CAA}{R}(1 + \frac{C_2\nu_{xz}}{2})] + E_x h \cdot CAA \cdot (BB) \cdot$$
$$- \frac{C_2\nu_{xz} Hq}{2}[CAA \cdot \frac{h}{R}(1 + \frac{C_2\nu_{xz}}{2}) - 3 \cdot CAA + h] \tag{3.12}$$

$$M = CA \cdot \{\frac{E_x h}{R}(1 + \frac{C_2\nu_{xz}}{2})\,(AA) - E_x h \cdot BB + \frac{C_2\nu_{xz}}{2} Hq\,[\frac{h}{R}(1 + \frac{C_2\nu_{xz}}{2}) - 3]\} \tag{3.13}$$

where

$$CA = 1/[\frac{1}{R^2}(1 + \frac{C_2\nu_{xz}}{2})\,(1 + C_2\nu_{xz}) - \frac{12}{h^2}]$$

$$CAA = CA \cdot (1 + C_2\nu_{xz})/R$$

$$AA = \varepsilon_x^o + \frac{h^2}{12} K_x' + \frac{h^4}{4!\cdot 80} K_x^{iv} + \frac{h^6}{6!\cdot 448} K_x^{v}$$

$$BB = K_x + \frac{3h^2}{3!\cdot 20} K_x'' + \frac{3h^4}{5!\cdot 112} K_x^{iv}$$

The coefficient of $\delta V$ gives

$$V = \frac{5Gh}{6}(\gamma_{xz}^o + \frac{h^2}{40} K_{xz}') = \frac{5Gh}{6} \cdot CC \tag{3.14}$$

where

$$CC = \gamma_{xz}^o + \frac{h^2}{40} K_{xz}'$$

Equations (3.10) through (3.14) are the stress resultant-displacement relations.

The coefficients of $\delta u$, $\delta u'$, $\delta w$, $\delta S$ and $\delta T$, in this case yield the five equilibrium equations. These are

$$N_{,x} + \frac{V}{R} = 0 \tag{3.15}$$

$$M_{,x} - V = 0 \tag{3.16}$$

$$N\left[-\frac{1}{R}+w_{,xx}+w_{o,xx}+\frac{h^2}{24}w_{,xx}''-\frac{h^2C_1}{12R}w_{,xx}'+\frac{C_1h^2}{12R^2}(w_{,xx}+w_{o,xx})+\frac{C_1h^4}{160R^2}w_{,xx}''\right]$$

$$+N_{,x}\left[w_{,x}+w_{o,x}+\frac{h^2}{24}w_{,x}''-\frac{C_1h^2}{12R}w_{,x}+\frac{C_1h^2}{12R^2}(w_{,x}'+w_{o,x})+\frac{C_1h^4}{160R^2}w_{,x}''\right]$$

$$+M\left[-\frac{C_1}{R}(w_{,xx}+w_{o,xx})+w_{,xx}'-\frac{3C_1h^2}{40R}w_{,xx}''+\frac{3C_1h^2}{40R^2}w_{,xx}'\right]$$

$$+M_{,x}\left[-\frac{C_1}{R}(w_{,x}+w_{o,x})+w_{,x}'-\frac{3C_1h^2}{40R}w_{,x}''+\frac{3C_1h^2}{40R^2}w_{,x}'\right]$$

$$+V_{,x}+qH=0 \tag{3.17}$$

$$\frac{N}{E_xh}C_2\nu_{xz}\left(1-\frac{h^2}{28R^2\nu_{zx}}\right)+\frac{M}{E_xh^2}\frac{C_2\nu_{xz}h}{R\nu_{zx}}\left(\frac{6}{5}+\frac{3h^2}{70R^2}\right)-\frac{C_2\nu_{xz}}{2E_x\nu_{zx}}\left(1-\frac{6hC_1}{35R}\right.$$

$$+\frac{h^2C_1}{20R^2}Hq+C_2\,\varepsilon_z^o=0 \tag{3.18}$$

$$\frac{N}{E_xh}\frac{C_2\nu_{xz}h}{12R\nu_{zx}}\left(\frac{1}{7}+\frac{h^2}{84R^2}\right)+\frac{M}{E_xh^2}\frac{C_2\nu_{xz}}{5}\left(1-\frac{h^2}{14R^2\nu_{zx}}\right)-\frac{C_2\nu_{xz}}{20E_x\nu_{zx}}\left[\frac{4}{7}-\frac{h}{6R}\right.$$

$$\left.+\frac{h^2}{18R^2}\right]Hq+\frac{C_2h}{60}K_z=0 \tag{3.19}$$

From (3.16)

$$V=M_{,x} \tag{3.16a}$$

Substituting (3.16a) into (3.15), we get

$$N_{,x}+\frac{1}{R}M_{,x}=0 \tag{3.15a}$$

or

$$N_{,x}=-\frac{1}{R}M_{,x} \tag{3.15b}$$

Substituting (3.15b) and (3.16a) into (3.17), we get

$$N\cdot\left[-\frac{1}{R}+(CD)_{,x}\right]+M_{,x}\cdot\left[(CE)-\frac{1}{R}(CD)\right]+M\cdot\left[(CE)_{,x}\right]+M_{,xx}+qH=0 \tag{3.17a}$$

where

$$CD=w_{,x}+w_{o,x}+\frac{h^2}{24}w_{,x}''-\frac{h^2C_1}{12R}w_{,x}'+\frac{C_1h^2}{12R^2}(w_{,x}+w_{o,x})+\frac{C_1h^4}{160R^2}w_{,x}''$$

$$CE = -\frac{C_1}{R}(w_{,x} + w_{o,x}) + w_{,x}' - \frac{3C_1h^2}{40R} w_{,x}'' + \frac{3C_1h^2}{40R^2} w_{,x}'$$

Equations (3.15b), (3.16), (3.17a), (3.18) and (3.19) are the equilibrium equations.

The natural boundary condition terms are

$$\begin{aligned}
&[[\delta u\,[N] + \delta u'\,[M] + \delta w\,[(N + \frac{h^2C_1}{12R^2}N - \frac{1}{R}M)\,(w_{,x} + w_{o,x}) \\
&\quad + (M - \frac{C_1h^2}{12R}N + \frac{3C_1h^2}{40R^2}M)\,w_{,x}' + (\frac{h^2}{24}N - \frac{3C_1h^2}{40R}M + \frac{C_1h^4}{160R^2}N)\,w_{,x}''] \\
&\quad + \delta w'[(M - \frac{h^2}{12}N + \frac{3h^2C_1}{40R^2}M)\,(w_{,x} + w_{o,x}) + (\frac{h^2}{24}N - \frac{3h^2}{20}M - \frac{h^4}{80R}N)\,w_{,x}' \\
&\quad + (\frac{3h^2}{40}M - \frac{C_1h^4}{160R}N + \frac{3C_1h^4}{224R^2}M)\,w_{,x}''] + \delta w''[(\frac{h^2}{24}N - \frac{3C_1h^2}{40R}M + \frac{C_1h^4}{160R^2}N) \\
&\quad \cdot (w_{,x} + w_{o,x}) + (\frac{3h^2}{40}M - \frac{C_1h^4}{160R}N + \frac{3C_1h^4}{224R^2}M)\,w_{,x}' + \frac{h^4}{320}N\,w_{,x}'' - \frac{3C_1h^4}{448R}M \\
&\quad + \frac{C_1h^6}{3584R^2}N)\,w_{,x}'' + \frac{h^2}{40}V]\,]]_0^L
\end{aligned} \tag{3.20}$$

They are in the form of stress, displacement or mixed boundary conditions. For example, we have for the first term, either u prescribed or $N = N^*$ (constant) prescribed at $x = 0$ and L.

## III.4. Non-dimensionalized Equations

Let us introduce the following non-dimensional variables:

$$x = Ls, \qquad u = \frac{h^2}{L}\phi, \qquad u' = \frac{h}{L}\psi$$

$$w = h\alpha, \qquad w' = \frac{h}{L}\beta, \qquad W'' = \frac{h}{L^2}\gamma$$

$$w_o = h\,\overline{w}_o \qquad \lambda = L^2/Rh$$

and $(\frac{h}{L})^n = p^n$ where n is an integer.

Then the abbreviated constants and functions are

$$\overline{CA} \equiv \frac{CA}{h^2} = \frac{1}{p^4 \cdot \lambda^2 \cdot (1 + \frac{C_2 \nu_{xz}}{2})\ (1 + C_2 \nu_{xz}) - 12} \tag{3.21}$$

$$\overline{CAA} = \frac{CAA}{h} = \frac{\lambda \cdot p^2 \cdot (1 + C_2 \nu_{xz})}{p^4 \cdot \lambda^2 \cdot (1 + \frac{C_2 \nu_{xz}}{2})\ (1 + C_2 \nu_{xz}) - 12} \tag{3.22}$$

$$\overline{H} = 1 + \frac{C_2}{2} \cdot \lambda \cdot p^2 \tag{3.23}$$

$$\begin{aligned}\overline{AA} = \frac{AA}{p^2} = {} & \phi_{,s} + \lambda \cdot \alpha + \frac{1}{2} \alpha_{,s}^2 + \overline{w}_{o,s}\, \alpha_{,s} + \frac{1}{24} p^2 \cdot (\lambda\gamma + \beta_{,s}^2 \\ & + \alpha_{,s}\, \gamma_{,s} - 2C_1\, \lambda \cdot p^1 \cdot \alpha_{,s}\, \beta_{,s} + C_1\, \lambda^2 \cdot p^2\, \alpha_{,s}^2 + 2C_1\, \lambda^2 \cdot p^2 \\ & \cdot \overline{w}_{o,s}\, \alpha_{,s} - 2C_1 \cdot \lambda \cdot p^1 \cdot \overline{w}_{o,s}\, \beta_{,s} + \overline{w}_{o,s}\, \gamma_{,s}) + \frac{1}{80} p^4 \cdot (\frac{1}{8} \gamma_{,s}^2 - \frac{C_1}{2} \lambda \\ & \cdot p^1 \cdot \beta_{,s}\, \gamma_{,s} - \frac{C_1}{2} \lambda^2\, p^2 \cdot \beta_{,s}^2 + \frac{C_1}{2} \lambda^2 \cdot p^2 \cdot \alpha_{,s}\, \gamma_{,s} + \frac{C_1}{2} \lambda^2 \\ & \cdot p^2 \cdot \overline{w}_{o,s}\, \gamma_{,s}) + \frac{C_1}{3584} \lambda^2 \cdot p^8 \cdot \gamma_{,s}^2\end{aligned} \tag{3.24}$$

$$\begin{aligned}\overline{BB} = \frac{h \cdot BB}{p^2} = {} & \psi_{,s} + \lambda \cdot p^1 \cdot \beta - \frac{C_1}{2} \lambda \cdot p^2 \cdot \alpha_{,s}^2 + p^1 \cdot \alpha_{,s}\, \beta_{,s} + p^1 \\ & \cdot \overline{w}_{o,s}\, \beta_{,s} - C_1 \cdot \lambda \cdot p^2 \cdot \overline{w}_{o,s}\, \alpha_{,s} + \frac{3}{20} \cdot p^3 \cdot (\frac{1}{2} \beta_{,s}\, \gamma_{,s} - \frac{C_1}{2} \lambda \\ & \cdot p^1 \cdot \beta_{,s}^2 - \frac{C_1}{2} \lambda \cdot p^1 \cdot \alpha_{,s}\, \gamma_{,s} + C_1\, \lambda^2 \cdot p^2 \cdot \alpha_{,s}\, \beta_{,s} + C_1\, \lambda^2 \\ & \cdot p^2 \cdot \overline{w}_{o,s}\, \beta_{,s} - \frac{C_1}{2} \lambda \cdot p^1 \cdot \overline{w}_{o,s}\, \gamma_{,s}) + \frac{3}{112} p^5 \cdot (- \frac{C_1}{8} \lambda \gamma_{,s}^2 \\ & + \frac{C_1}{2} \lambda^2 \cdot \beta_{,s}\, \gamma_{,s})\end{aligned} \tag{3.25}$$

$$\overline{CC} = \frac{CC}{p^1} = -p^2 \cdot \lambda \cdot \phi + \psi + \alpha_{,s} + \frac{1}{40} p^2\, \gamma_{,s} \tag{3.26}$$

$$\begin{aligned}\overline{CD} = \frac{CD}{p^1} = {} & \alpha_{,s} + \overline{w}_{o,s} + \frac{1}{24} p^2 \cdot \gamma_{,s} - \frac{C_1}{12} \cdot \lambda \cdot p^3 \cdot \beta_{,s} + \frac{C_1}{12} \lambda^2 \cdot p^4 \\ & \cdot (\alpha_{,s} + \overline{w}_{o,s}) + \frac{C_1}{160} \lambda^2 \cdot p^6 \cdot \gamma_{,s}\end{aligned} \tag{3.27}$$

$$\begin{aligned}\overline{CE} = \frac{CE \cdot h}{p^1} = {} & p^1\, [- C_1\, \lambda\, p^1 \cdot (\alpha_{,s} + \overline{w}_{o,s}) + \beta_{,s} - \frac{3C_1}{40} \lambda \cdot p^3 \cdot \gamma_{,s} \\ & + \frac{3C_1}{40} \lambda^2 \cdot p^4 \cdot \beta_{,s}]\end{aligned} \tag{3.28}$$

and the stress resultants are

$$\overline{N} = \frac{N}{E_x h} = \overline{AA} \cdot p^2 \cdot [1 - \lambda \cdot \overline{CAA} \cdot p^2 \cdot (1 + \frac{C_2 \nu_{xz}}{2})] + \overline{CAA} \cdot \overline{BB} \cdot p^2$$

$$- \frac{C_2 \nu_{xz}}{2} \overline{H} \cdot [\overline{CAA} \cdot p^2 \cdot \lambda \cdot (1 + \frac{C_2 \nu_{xz}}{2}) - 3 \cdot \overline{CAA} + 1] \frac{q}{E_x}$$

$$= \overline{DA} \cdot p^2 \cdot \overline{AA} + \overline{CAA} \cdot p^2 \cdot \overline{BB} - \overline{DB} \cdot \overline{q} \tag{3.29}$$

$$\overline{M} = \frac{M}{E_x h^2} = \overline{CA} \{p^4 \cdot \lambda \cdot (1 + \frac{C_2 \nu_{xz}}{2}) \overline{AA} - p^2 \cdot \overline{BB} + \frac{C_2 \nu_{xz}}{2} \overline{H}$$

$$\cdot [p^2 \cdot \lambda \cdot (1 + \frac{C_2 \nu_{xz}}{2}) - 3] \frac{q}{E_x}\}$$

$$= \overline{DC} \cdot p^2 \cdot \overline{AA} - \overline{CA} \cdot p^2 \cdot \overline{BB} - \overline{DE} \cdot \overline{q} \tag{3.30}$$

$$\overline{V} = \frac{V}{E_x h} = \frac{5G}{6E_x} p^1 \cdot [- p^2 \cdot \lambda \cdot \phi + \psi + \alpha_{,s} + \frac{p^2}{40} \gamma_{,s}]$$

$$= \overline{DF} \cdot p^1 \cdot \overline{CC} \tag{3.31}$$

$$\overline{S} = \frac{S}{E_x h} = - p^2 \cdot \lambda \cdot \overline{M} \tag{3.32}$$

$$\overline{T} = \frac{T}{E_x h} = - \frac{5}{2} p^2 \cdot \lambda \cdot \overline{N} + \frac{3}{2} \overline{H} \cdot \overline{q} \tag{3.33}$$

where

$$\overline{DA} = 1 - \lambda \cdot \overline{CAA} \cdot p^2 \cdot (1 + \frac{C_2 \nu_{xz}}{2})$$

$$\overline{DB} = \{\overline{CAA} \cdot [p^2 \cdot \lambda \cdot (1 + \frac{C_2 \nu_{xz}}{2}) - 3] + 1\} \cdot \frac{C_2 \nu_{xz}}{2} \overline{H}$$

$$\overline{DC} = \overline{CA} \cdot p^2 \cdot \lambda \cdot (1 + \frac{C_2 \nu_{xz}}{2})$$

$$\overline{DE} = - \overline{CA} \cdot \frac{C_2 \nu_{xz}}{2} \overline{H} \cdot [p^2 \cdot \lambda \cdot (1 + \frac{C_2 \nu_{xz}}{2}) - 3]$$

$$\overline{q} = \frac{q}{E_x}$$

$$\overline{DF} = \frac{5G}{6E_x}$$

With these expressions, the non-dimensional equations are:

(i) $\overline{DG} \cdot (\overline{AA})_{,s} + \overline{DH} \cdot (\overline{BB})_{,s} = 0$ (3.34)

where

$$\overline{DG} = \overline{DA} + \lambda \cdot p^2 \cdot \overline{DC} \text{ and } \overline{DH} = \overline{CAA} - p^2 \cdot \lambda \cdot \overline{CA}$$

(ii) $\overline{DC} \cdot p^2 \cdot (\overline{AA})_{,s} - \overline{CA} \cdot p^2 \cdot (\overline{BB})_{,s} - \overline{DF} \cdot \overline{CC} = 0$ (3.35)

(iii) $\overline{AA} \cdot [\overline{DA} \cdot (-\lambda + \overline{CD}_{,s}) + \overline{DC} \cdot \overline{CE}_{,s}] + \overline{BB} \cdot [\overline{CAA} \cdot (-\lambda + \overline{CD}_{,s})$
$- \overline{CA} \cdot \overline{CE}_{,s}] + \overline{AA}_{,s} \cdot \overline{DC} \cdot (\overline{CE} - \lambda \cdot p^2 \cdot \overline{CD}) - \overline{BB}_{,s} \cdot \overline{CA}$
$\cdot (\overline{CE} - \lambda \cdot p^2 \cdot \overline{CD}) + \overline{AA}_{,ss} \cdot \overline{DC} - \overline{BB}_{,ss} \cdot \overline{CA} + [\overline{H} - \overline{DB}$
$\cdot p^2 \cdot (-\lambda + \overline{CD}_{,s}) - \overline{DE} \cdot p^2 \cdot \overline{CB}_{,s}] \cdot Q = 0$ (3.36)

where $Q = \dfrac{\overline{q}}{p^4}$

(iv) $\overline{DL} \cdot \overline{AA} + \overline{DM} \cdot \overline{BB} + \overline{DN} \cdot Q + \beta = 0$ (3.37)

where

$$\overline{DL} = (\overline{DI} \cdot \overline{DA} + \overline{DJ} \cdot \overline{DC}) \cdot p^1$$

$$\overline{DM} = (\overline{DI} \cdot \overline{CAA} - \overline{DJ} \cdot \overline{CA}) \cdot p^1$$

$$\overline{DN} = (\overline{DK} - \overline{DB} \cdot \overline{DI} - \overline{DJ} \cdot \overline{DE}) \cdot p^3$$

$$\overline{DI} = C_2 \cdot \nu_{xz} - \frac{C_2\lambda^2}{28} p^4 \cdot pR$$

$$\overline{DJ} = \frac{3}{5} C_2 \cdot pR \cdot p^2 \cdot \lambda \cdot (2 + \frac{p^4}{14} \cdot \lambda^2)$$

$$\overline{DK} = \frac{C_2}{2} \overline{H} \cdot pR \cdot (-1 + \frac{6\lambda}{35} \cdot p^2 - \frac{1}{20} \lambda^2 \cdot p^4) \cdot p^4$$

$$pR = \nu_{xz}/\nu_{zx}$$

(v) $\overline{DS} \cdot \overline{AA} + \overline{DT} \cdot \overline{BB} - \overline{DU} \cdot p^2 \cdot Q + \gamma = 0$ (3.38)

where

$$\overline{DP} = C_2 \cdot pR \cdot p^2 \cdot \lambda \cdot (\frac{5}{7} + \frac{5}{84} p^4 \cdot \lambda^2)$$

$$\overline{DQ} = 12C_2 \cdot \nu_{xz} \cdot (1 - \frac{p^4}{14\nu_{zx}} \lambda^2)$$

$$\overline{DR} = \frac{3C_2}{2} pR \cdot \overline{H} (-\frac{8}{7} + \frac{\lambda}{3} \cdot p^2 - \frac{\lambda^2}{9} p^4)$$

$$\overline{DS} = \overline{DP} \cdot \overline{DA} + \overline{DQ} \cdot \overline{CA}$$

$$\overline{DT} = \overline{DP} \cdot \overline{CAA} - \overline{DQ} \cdot \overline{CA}$$

$$\overline{DU} = \overline{DP} \cdot \overline{DB} + \overline{DQ} \cdot \overline{DE} - \overline{DR}$$

In deriving the last two equations (3.37) and (3.38), we take $C_2 = 1$ (for the last terms in both equations) in order that the equations are nonvanishing (i.e. the coefficient matrix is nonsingular). This is for the case of neglecting transverse normal stress ($C_2 = 0$) and the solutions $\beta = 0$ and $\gamma = 0$ are obtained.

## III.5. Comparison of Three Theories

When we set $C_2 = \beta = \gamma = 0$ in (3.34) through (3.38), the equations are specialized into those of shear deformation theory with the modification in the Euler-Bernoulli type theorem. If we completely neglect z/R terms ($C_1 = 0$) as well as imperfection terms ($w_0 = 0$) the following shear theory is obtained:

$$\text{(a)}\quad \phi_{,ss} + \lambda \cdot \alpha_{,s} + \alpha_{,s}\,\alpha_{,ss} = 0 \tag{3.39}$$

$$\text{(b)}\quad \frac{p^4 \cdot \lambda}{p^4 \cdot \lambda^2 - 12}\left(\phi_{,ss} + \lambda \cdot \alpha_{,s} + \alpha_{,s}\,\alpha_{,ss}\right) - \frac{p^2}{p^4 \cdot \lambda^2 - 12}\,\psi_{,ss} - \frac{5}{6}\frac{G}{E_x}\left(-p^2 \cdot \lambda \cdot \phi + \psi + \alpha_{,s}\right) = 0 \tag{3.40}$$

$$\text{(c)}\quad \frac{12}{p^4 \cdot \lambda^2 - 12}\left(\lambda - \alpha_{,ss}\right)\left(\phi_{,s} + \lambda \cdot \alpha + \frac{1}{2}\alpha_{,s}^2\right) - \frac{\lambda \cdot p^2}{p^4 \cdot \lambda^2 - 12}\left(\lambda - \alpha_{,ss}\right)\psi_{,s} - \frac{p^4 \cdot \lambda^2}{p^4 \cdot \lambda^2 - 12}\,\alpha_{,s}\left(\phi_{,ss} + \lambda \cdot \alpha_{,s} + \alpha_{,s}\,\alpha_{,ss}\right) + \frac{\lambda \cdot p^2}{p^4 \cdot \lambda^2 - 12} \cdot \alpha_{,s}\,\psi_{,ss} + \frac{p^2 \cdot \lambda}{p^4 \cdot \lambda^2 - 12}\left(\phi_{,sss} + \lambda \cdot \alpha_{,ss} + \alpha_{,s}\,\alpha_{,sss} + \alpha_{,ss}^2\right) - \frac{1}{p^4 \cdot \lambda^2 - 12}\,\psi_{,sss} + Q = 0. \tag{3.41}$$

These equations are to be compared to the equations for the shear deformation which if derived independently are

$$\text{(a)}\quad \phi_{,ss} + \lambda\alpha_{,s} + \alpha_{,s}\,\alpha_{,ss} + \frac{1}{12}p^2 \cdot \lambda \cdot \psi_{,ss} = 0$$

$$\text{(b)}\quad \frac{1}{12}p^2 \cdot \psi_{,ss} - \frac{G}{E_x}\left(-p^2 \cdot \lambda \cdot \phi + \psi + \alpha_{,s}\right) = 0$$

$$\text{(c)} \quad -(\lambda - \alpha,_{ss})\,(\phi,_s + \lambda \cdot \alpha + \frac{1}{2}\alpha,_s^2) - \frac{1}{12}p^2 \cdot \lambda \cdot \alpha,_s \cdot \psi,_{ss}$$

$$+ \frac{1}{12}\,\psi,_{sss} - Q = 0$$

The underlined terms are the differences in these two sets of equations. However the underlined terms all contain powers of h/L, i.e., $p^2$, $p^4$, etc. Thus the differences between the two sets becomes smaller as the arch becomes thinner. Further simplification of the equations as h/L approaches zero, leads to the classical equations for the arch, viz:

$$\text{(a)} \quad \phi,_{ss} + \lambda \cdot \alpha,_s + \alpha,_s\,\alpha,_{ss} = 0 \tag{3.42}$$

$$\text{(b)} \quad \psi + \alpha,_s = 0 \tag{3.43}$$

$$\text{(c)} \quad (\phi,_s + \lambda\,\alpha + \frac{1}{2}\alpha,_s^2)\,(\lambda - \alpha,_{ss}) - \frac{1}{12}\psi,_{sss} - Q = 0 \tag{3.44}$$

With the initial imperfections neglected, the first equation is identical to (2.18a) while combination of the last two equations is identical to (2.18b).

## III.6. Method of Solution

Let us employ the same method of linearization of the nonlinear equations as in the previous chapter. For boundary condition, the clamped end case of $\phi = \psi = \alpha = \beta = \gamma = 0$ at $s = 0$ and 1 are considered, since these displacement components can be rather easily specified. Because third order derivatives are involved in the third equation, forward and backward differences are used in order to avoid the values at nodal points outside the boundary, viz:

$$\Delta_s^3\,\alpha_i = \frac{D^3}{2}\,(-3\alpha_{i-1} + 10\alpha_i - 12\alpha_{i+1} + 6\alpha_{i+2} - \alpha_{i+3})$$

and

$$\nabla_s^3\,\alpha_i = \frac{D^3}{2}(\alpha_{i-3} - 6\alpha_{i-2} + 12\alpha_{i-1} - 10\alpha_i + 3\alpha_{i+1})$$

where $\Delta_s$ is the forward difference and $\nabla_s$ is the backward difference.

As in the last chapter, the equations are written in finite difference form. Deflection input in the computer program will be used to extend the load-deflection curve beyond the first peak. Therefore the additional equation

$$\text{AREA} = \frac{1}{\tilde{N}+1} \sum_{i=1}^{\tilde{N}} \alpha_i$$

is used.

The newly formed equation represents a system of $(5\tilde{N} + 1)$ simultaneous nonlinear algebraic equations which are solved by Newton's iteration scheme. The polynomial in section II.4. is also used as for the antisymmetric initial imperfection.

The orthotropic elastic constants are taken from reference [22] as

$$E_x = 4.20 \times 10^6 \text{ psi}$$

$$E_z = 10.20 \times 10^6 \text{ psi}$$

$$G = 2.7 \times 10^6 \text{ psi}$$

$$\nu_{xz} = 0.11$$

$$\nu_{zx} = 0.26$$

where the relation $E_x\nu_{zx} = E_z\nu_{xz}$ is approximately satisfied.

III.7. Discussion of Results

Theories of varying degrees of accuracy may be obtained as special cases of the general theory which considers transverse normal stress and shear deformation. For the limiting point "a" as well as the bifurcation point "b" (Fig. 8), the more accurate the theory, the lower the critical load is found to be. The load-central deflection curves for $\lambda = 56.7$ are shown in Fig. 8 and their enlarged upper portions are shown in Fig. 9. The discrepancy in critical load for the classical theory developed in the last chapter and the

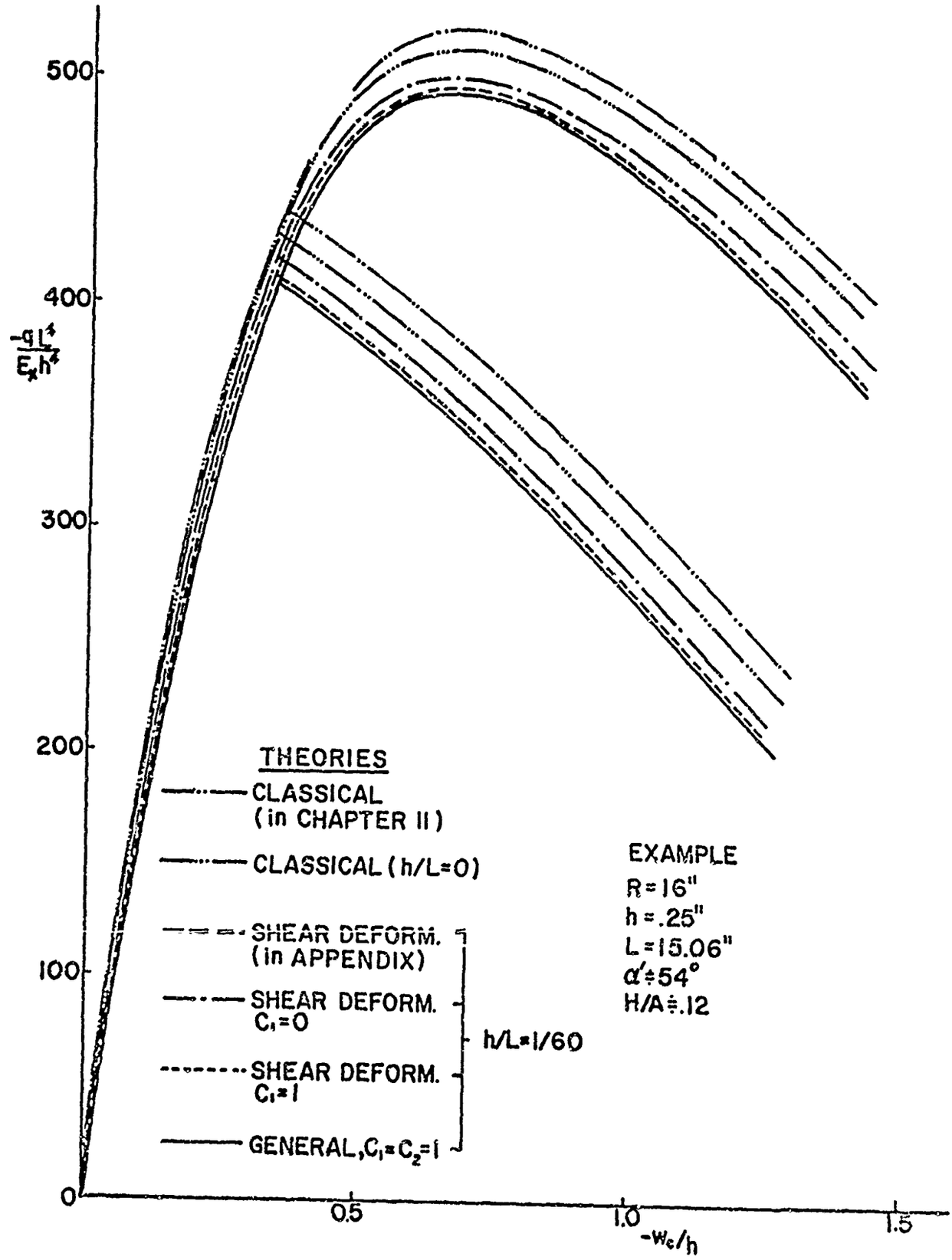


FIG. 8 LOAD-DEFLECTION CURVES FOR VARIOUS THEORIES — $\lambda=56.7$

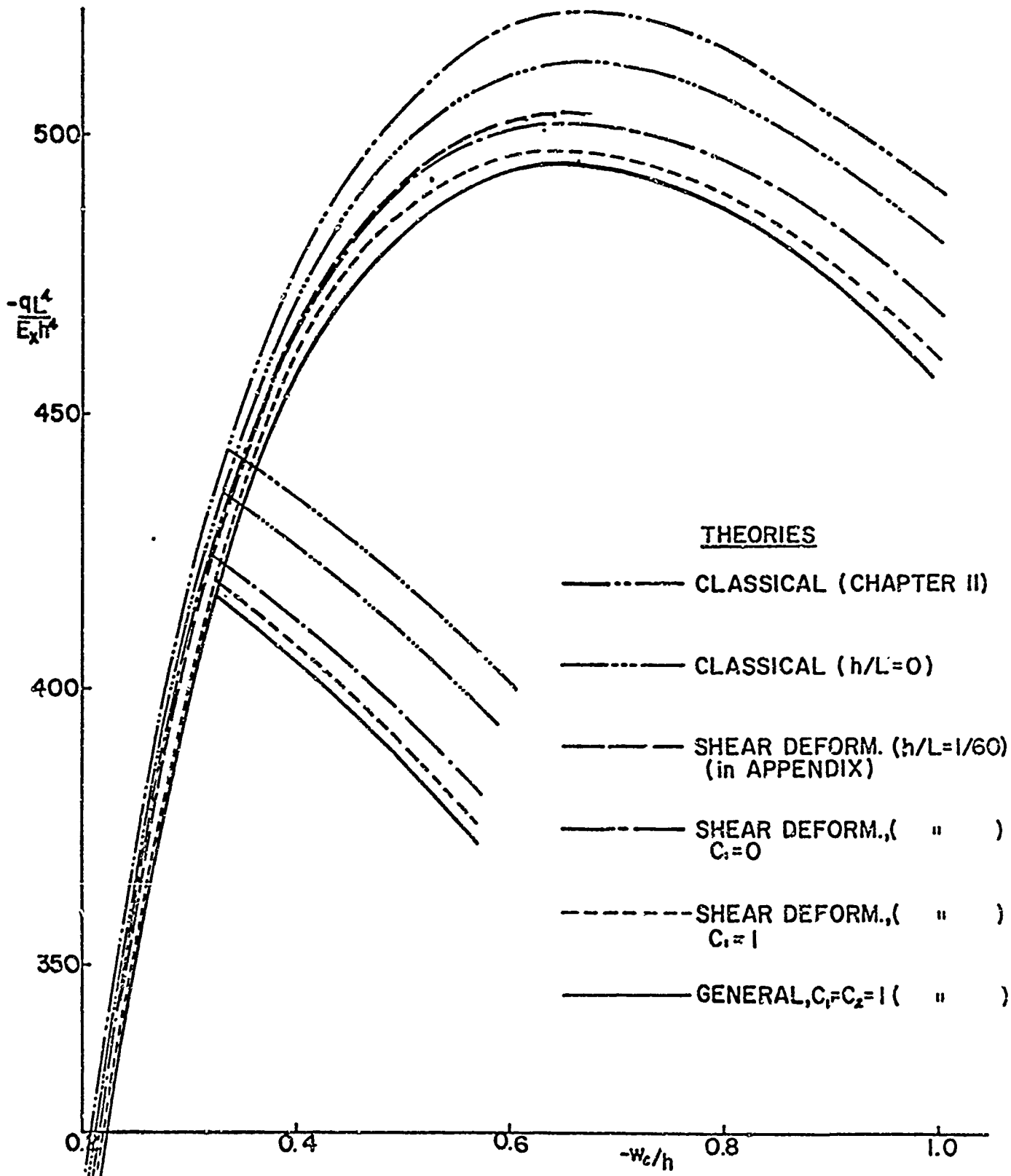


FIG. 9 COMPARISON OF VARIOUS THEORIES—$\lambda=56.7$
(UPPER PORTION OF FIG. 9)

one obtained as a special case from the general theory is about 1.3 percent of the latter. This discrepancy is a result of a different network of grid points involved in the finite difference formulation of the fourth order derivative in equation (2.18b) and the combination of first and third order derivatives in (3.43) and (3.44) respectively. For comparative purposes, all theories will be compared to the classical type theory obtained as a special case from the general theory which includes transverse shear as well as transverse normal stress effects. For h/L = 1/60, the asymmetric critical load corresponding to classical theory is about 4.3 percent higher than that found when the transverse normal stress and shear deformation theory is employed. Also the load found from modified shear deformation theory ($C_2 = \beta = \gamma = 0$) is only 0.7 percent greater than the general theory. The shear deformation theory ($C_1 = C_2 = \beta = \gamma = 0$) runs 1 percent higher than the modified shear deformation theory. Similar results are obtained for $\lambda = 35.0$ as shown in Fig. 10.

The shear effects become very significant when the arch is moderately thick. For $\lambda = 13$, h/L = 1/13.3 as shown in Fig. 11, the critical load found from classical theory is 16 percent greater than that found when normal stress and shear are considered. However the difference between results obtained from the modified shear theory and the normal stress and shear theory is usually less than 2 percent. In this case the shear deformation theory (with $C_1 = C_2 = \beta = \gamma = 0$) is not adequate to describe the behavior of the arch since the critical load is about 8 percent higher than that found from the modified shear deformation theory ($C_1 \neq 0$).

The comparison of the critical loads found from the classical as well as the shear and normal stress theories is shown in Fig. 12. The percentage difference between results obtained from the former and the latter theories is noted.

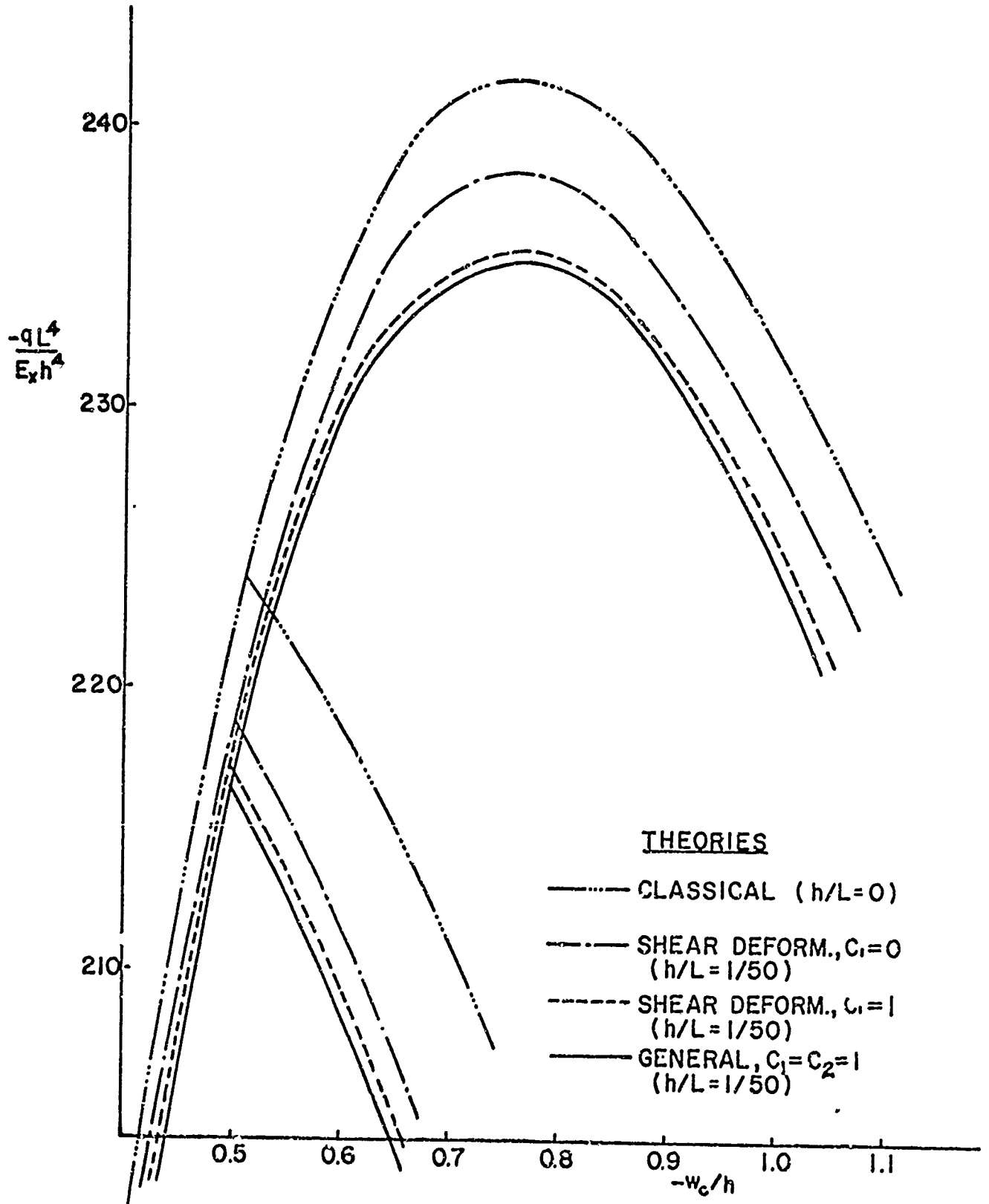


FIG. 10 UPPER PORTION OF LOAD-DEFLECTION CURVES—$\lambda=35$

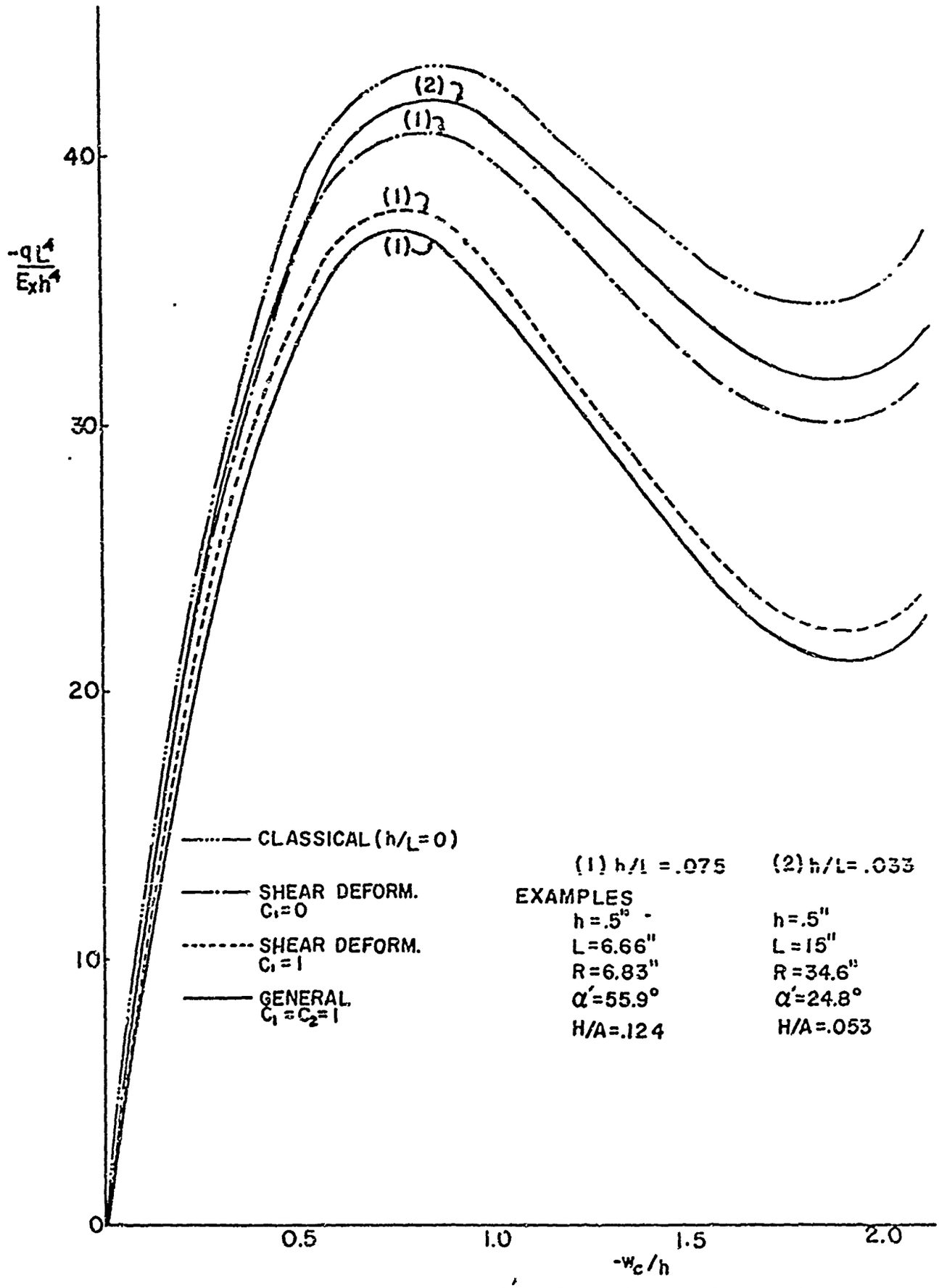


FIG. 11 LOAD DEFLECTION CURVES FOR MODERATELY THICK ARCH
$\lambda = 13$

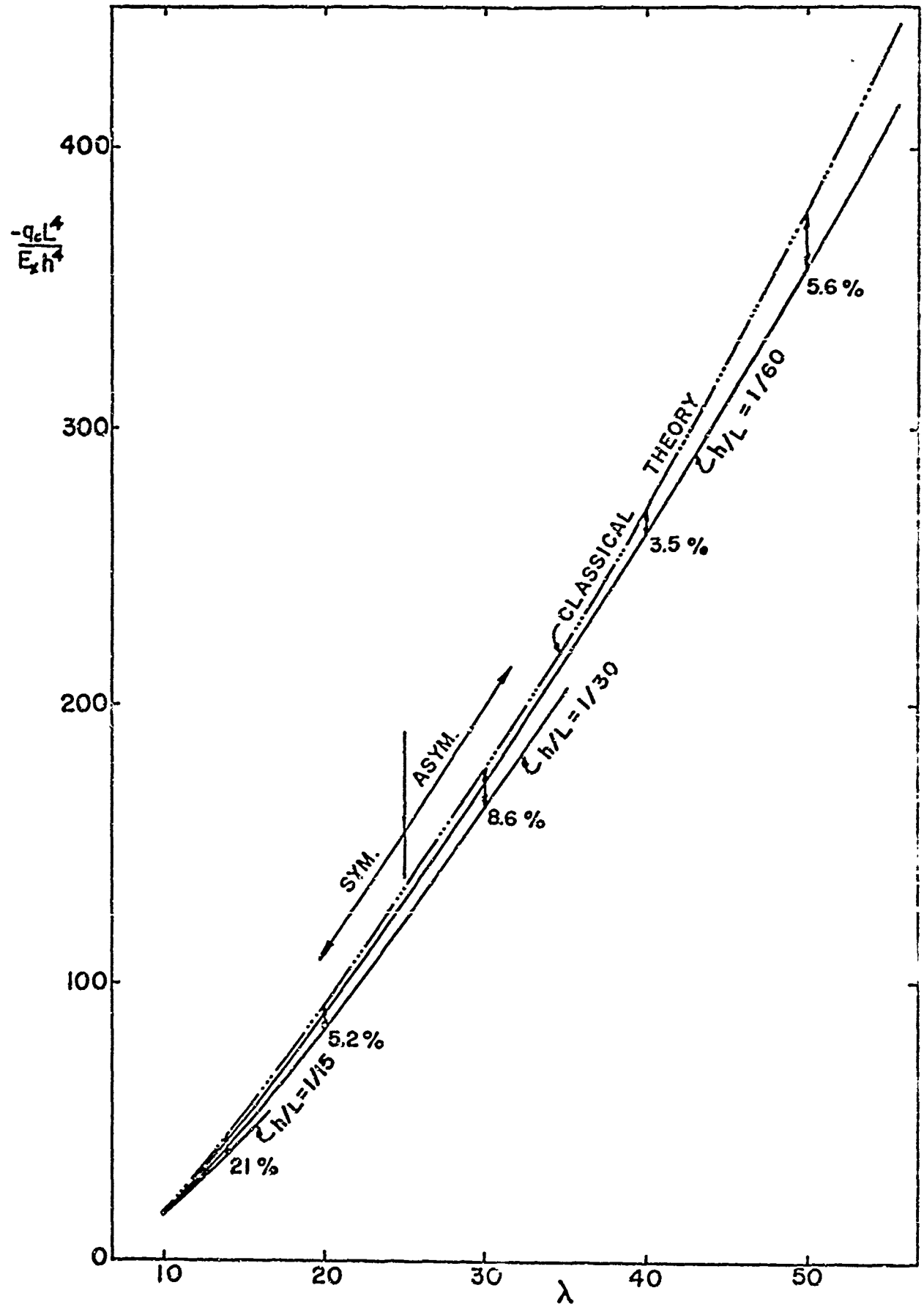


FIG. 12 COMPARISON BETWEEN CLASSICAL AND GENERAL THEORIES

# CHAPTER IV

# EXPERIMENTS ON RADIALLY REINFORCED ARCHES

## IV.1. Introduction

Experiments were carried out on arches composed of resin matrices in which were embedded small diameter glass fibers each oriented toward the center of curvature of the arch. This type of construction was first produced for laboratory purposes by Uniroyal, Inc. [23]. The nature of this composite material makes it well-suited to withstand loadings normal to its convex surface. Such loadings would occur in deep submergence pressure hulls. Evidently during hydrostatic loading both the resin matrix as well as the glass fibers are acting in compression and the resin is restrained from extrusion from between the glass rods by shear coupling, thus placing the glass filaments in a state of axial tension. It has been demonstrated that spherical shells constructed of such radially oriented reinforcement have extremely desirable weight/displacement relations [24].

The objective of the present experiments is to investigate validity of the various theories developed earlier in the present investigation.

## IV.2. Fabrication of the Material

Fabrication of the radially reinforced arches was carried out in accordance with the following procedure:

(a) Material: The material utilized high strength S glass roving embedded in an epoxy resin which is marketed through Minnesota Mining and Manufacturing Co. under the designation of 1009-26-S which is a glass impregnated tape one inch wide and 500 feet in length. The glass fibers are of course oriented in the 500 foot direction. The tape is cut into short lengths each corresponding to the desired thickness of the arch, in this case 0.25 inches.

(b) Curing: To build small mosaic-type curved blocks, the 0.25 inch lengths of tape were stacked into a curved mold having a 16 inch radius of curvature. A spring force in the direction of the arch middle-surface was applied so as to develop a pressure of 2000 $lb/in^2$ to compact the short lengths of tape. Holes were provided in the mold to permit escape of excess resin. The mold was then placed in a small oven and the mosaic block cured at temperatures of 300°F to 325°F for 30 minutes. The cured block contained about 80 percent glass.

(c) Post-curing: The cured mosaic-type blocks were joined to one another by an epoxy of minimum thickness so as not to influence the resin content of the resulting arch. The entire assembly was then placed in a larger mold and cured again at 350°F to 375°F for four hours.

In addition to arches constructed by the above technique, additional specimens were provided by Uniroyal, Inc. The physical properties of the resulting composite are described in [22] and Fig. 13(a) illustrates the nature of the material.

IV.3. Description of Test Apparatus

The test apparatus consists of a loading fixture which includes end supports for the arch as well as a system to provide lateral pressure on the convex surface of the arch. Also, a system of transducers for measuring displacements was developed.

(a) Support conditions: The ends of the arch were clamped by means of two metal blocks tightened around the arch by means of two bolts. One of these bolts went through the end of the arch. It was believed that this corresponds reasonably well to a clamped end condition, as illustrated in Fig. 13(a). A slot corresponding to the curvature of the arch was milled into the blocks so as to provide good clamping. This technique for simulating a clamped

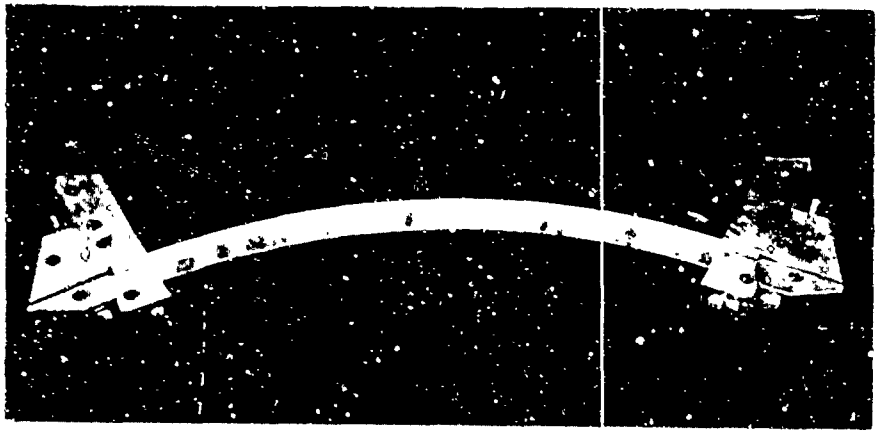

(a) SAMPLE OF RADIAL FILAMENT ARCH WITH CLAMPED SUPPORTS

(b) THE ARCH ASSEMBLY AND THE DATA RECORDING SYSTEM

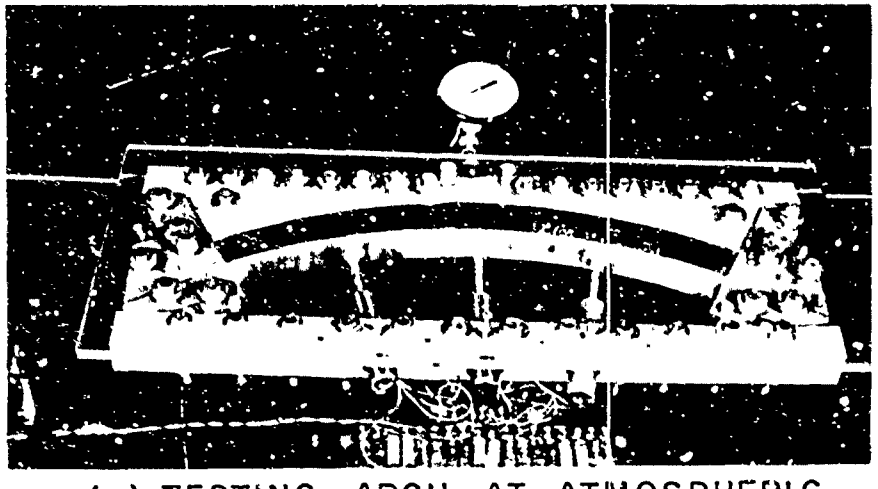

(c) TESTING ARCH AT ATMOSPHERIC PRESSURE

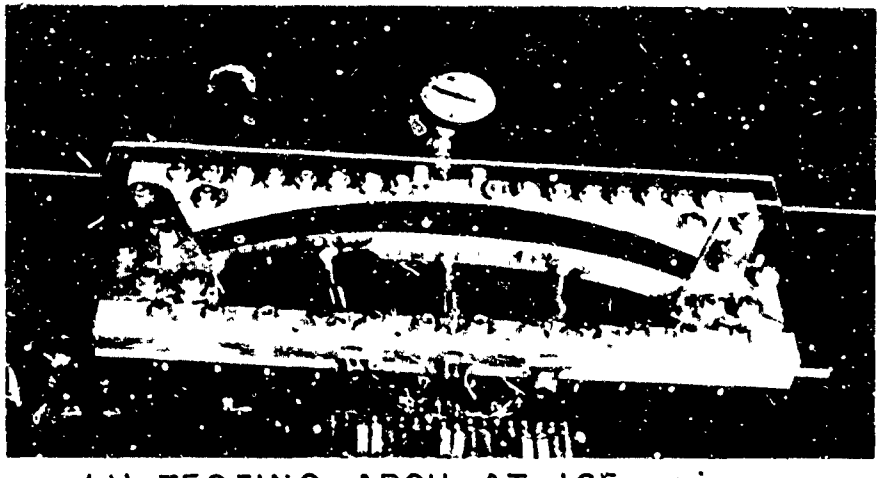

(d) TESTING ARCH AT 165 p.s.i. PRESSURE (RIGHT BEFORE ARCH COLLAPSE)

Figure 13

end was first tested for a straight cantilever beam and found to lead to deflections in good agreement with simple beam theory. On this basis it was considered a good representation of a clamped end condition.

(b) Deformation measurement system: Radial displacements were monitored by use of three Schaevitz Linear Variable differential transformers, Type 300-SSLT, henceforth designated LVDT. These units each has a range of ± 0.3 inches with a linearity larger than ± 1 percent of the full range output. Each LVDT consists of a three winding transformer together with a removable core as illustrated in Fig. 14(a). When the core is centered with respect to the two secondary windings the induced voltages $V_1$ and $V_2$ are equal. As the core is displaced toward either secondary winding that induced voltage increases whereas that from the other secondary winding decreases. When the core is attached to the arch the radial displacement of the arch can be monitored. With the aid of some additional circuitry the interpretation of resulting data can be made easier. The circuit corresponding to this is shown in Fig. 14(b). With the core in the central position the output voltage $V_0$ is equal to zero and as the core moves positively the voltage increases positively and vice versa. For full core displacement of ± 0.3 inches the output voltage changes by approximately ± 3 volts for a 6.3 volt excitation of the primary.

The arch displacements treated were of the order of magnitude of the arch thickness, i.e. 0.25 inches. It was anticipated that the maximum radial displacement would be no more than 0.5 inches. Because of this the core was attached to the arch after a positive displacement of 0.25 inches of the core had been imposed. This leads to a useful displacement range of 0.50 inches which is within

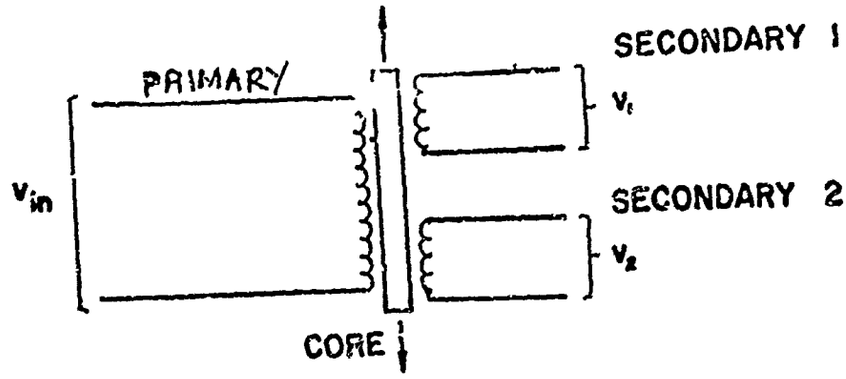


(a) LINEAR VARIABLE DIFFERENTIAL TRANSFORMER CONSISTS 3 WINDING TRANSFORMERS AND A CORE

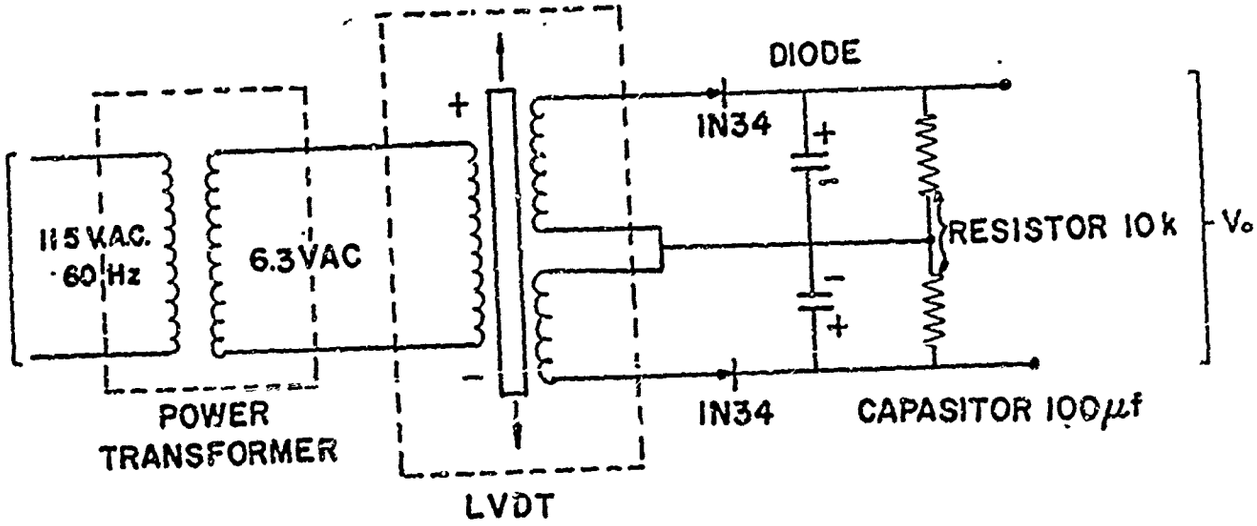


(b) ADDITIONAL CIRCUITRY TO MAKE INTERPRETATION EASIER

FIG. 14 LINEAR VARIABLE DIFFERENTIAL TRANSFORMER & CIRCUITRY

the linear range of action of the LVDT.

The output voltage $v_0$ was monitored by a Honeywell Visicorder, Type 2106 which displayed voltage changes on a six inch wide strip chart. The signal conditioning amplifiers were adjusted so that a core displacement of 0.5 inches (measured from the pre-set 0.25 inch position) gave a full five inch displacement on the chart paper. Thus, 0.1 inch of deflection on the chart corresponds to 0.01 inches of arch deflection.

(c) Pressure loading system: The pressure system consists of an oil jack, a pressure chamber, and a pressure gage.

(1) Pressure chamber: This was formed on the convex side of the arch by bounding that side by a concave shaped piece of hard wood together with two 0.5 inch thick plexiglass sheets, one on either side of the arch. The plexiglass sheets were bolted together through the hard wood as well as through the arch supports. A bicycle-type inner tube was placed in the space between the arch and the hard wood and connected to the oil jack. Uniform hydrostatic pressure was then applied to the convex side of the arch by pumping oil into the extremely flexible inner tube.

(2) Pressure gage: A gage manufactured by the U.S. Gage Co. and capable of monitoring pressures up to 200 $lb/in^2$ was connected between the inner tube and the oil jack. The gage was of course calibrated prior to testing the arches.

(3) Oil jack: A Hein-Werner Pushmaster Hydraulic Pump Unit Model FP-4 was employed. It was found that ordinary jack oil rather quickly damages the rubber in the inner tube so paraffin oil was employed.

## IV.4. Test Procedure

The cured arch was clamped in the metal blocks and this assembly surrounded by the plexiglass plates and hard wood backing for the inner tube. The core of each LVDT was epoxied to the concave surface of the arch. One transducer was located at each quarter point of the arch and one at the mid-point. Figs. 13(b) and (c) illustrate the test apparatus.

The output sides of the LVDT's were connected to the input side of the Honeywell Accudata 117 DC Amplifier and the LVDT's energized by means of a transformer operating from the 115 volt AC source. The amplifier was activated and the ultraviolet light beam centered on the chart paper. The gain was adjusted so as to keep the trace on the chart. With the aid of a micrometer the LVDT was displaced in the direction of the convex side of the arch by 0.25 inches and the LVDT locked in position.

Oil pressure was slowly applied while the Visicorder chart paper was driven at 0.5 inches/sec. LVDT readings were taken at 10 lb/in$^2$ increments until arch collapse occurred.

## IV.5. Test Results

Eleven arches were tested and the results are indicated in Table 1 and plotted as load-deflection diagrams in Fig. 15. This permits comparison between the various theoretical results obtained earlier in this study and experimental evidence.

Specimens 3, 9, and 10 possessed some slight imperfections in bonding of the various mosaic-type blocks into the arch configuration and accordingly exhibited lower strength characteristics than did better constructed specimens. Specimens 1, 2, 4, 5, 6, 7, and 11 collapsed into a nonsymmetric configuration upon buckling. For all of these specimens, collapse occurred in the neighborhood of 135 lb/in$^2$ or slightly more, which is in good agreement with theoretical predictions based upon an asymmetric buckling mode. A somewhat greater collapse pressure was found for Specimen 8. This arch

# TABLE 1 EXPERIMENTAL RECORDS

| SAMPLE NO. | | 1 | | 2 | | 3 | | 4 | | 5 | | 6 | | 7 | | 8 | | 9 | | 10 | | 11 | |
|---|---|---|---|---|---|---|---|---|---|---|---|---|---|---|---|---|---|---|---|---|---|---|---|
| Load, q psi | $\frac{qL^4}{E_s H^4}$ | $w_c$ IN | $\alpha_c$ | $w_c$ IN | $\alpha_c$ | $w_c$ IN | $\alpha_c$ | $w_c$ IN | $\alpha_c$ | $w_c$ IN | $\alpha_c$ | $w_c$ IN | $\alpha_c$ | $w_c$ IN | $\alpha_c$ | $w_c$ IN | $\alpha_c$ | $w_c$ IN | $\alpha_c$ | $w_c$ IN | $\alpha_c$ | $w_c$ IN | $\alpha_c$ |
| 10 | 30.85 | .004 | .016 | .005 | .020 | .004 | .016 | .007 | .028 | .002 | .008 | .004 | .016 | .005 | .020 | .004 | .016 | .003 | .012 | .010 | .040 | .005 | .020 |
| 20 | 61.70 | .008 | .032 | .010 | .040 | .008 | .032 | .015 | .060 | .004 | .016 | .007 | .028 | .010 | .040 | .007 | .028 | .006 | .024 | .020 | .080 | .010 | .040 |
| 30 | 92.70 | .012 | .048 | .016 | .064 | .013 | .052 | .023 | .092 | .006 | .024 | .011 | .044 | .015 | .060 | .013 | .050 | .009 | .036 | .030 | .120 | .016 | .064 |
| 40 | 123.50 | .016 | .064 | .022 | .088 | .020 | .080 | .031 | .124 | .010 | .040 | .015 | .060 | .020 | .080 | .020 | .080 | .012 | .048 | .040 | .160 | .022 | .088 |
| 50 | 154.50 | .026 | .104 | .032 | .128 | .030 | .120 | .038 | .152 | .014 | .056 | .021 | .084 | .025 | .100 | .029 | .115 | .018 | .072 | .058 | .232 | .027 | .108 |
| 60 | 185.00 | .036 | .144 | .042 | .168 | .038 | .152 | .045 | .180 | .020 | .080 | .028 | .112 | .030 | .120 | .035 | .140 | .025 | .100 | .075 | .300 | .032 | .128 |
| 70 | 216.00 | .042 | .168 | .050 | .200 | .050 | .200 | .052 | .208 | .030 | .120 | .038 | .152 | .035 | .140 | .045 | .180 | .035 | .140 | .095 | .380 | .038 | .152 |
| 80 | 247.00 | .048 | .192 | .057 | .228 | .060 | .240 | .060 | .240 | .038 | .152 | .048 | .192 | .040 | .160 | .047 | .190 | .046 | .184 | .115 | .460 | .044 | .176 |
| 90 | 278.00 | .057 | .228 | .065 | .260 | .070 | .280 | .071 | .284 | .050 | .200 | .057 | .228 | .050 | .200 | .069 | .290 | .050 | .200 | .142 | .568 | .053 | .212 |
| 100 | 308.50 | .066 | .264 | .075 | .300 | .080 | .320 | .082 | .328 | .060 | .240 | .066 | .264 | .060 | .240 | .090 | .360 | .054 | .216 | | | .062 | .248 |
| 110 | 340.00 | .077 | .308 | .085 | .340 | | | .093 | .372 | .080 | .320 | .080 | .320 | .070 | .280 | .110 | .440 | | | | | .073 | .292 |
| 120 | 370.00 | .090 | .360 | .100 | .400 | | | .105 | .420 | .100 | .400 | .094 | .376 | .080 | .320 | .135 | .540 | | | | | .085 | .340 |
| 130 | 402.00 | .124 | .496 | .118 | .472 | | | .130 | .520 | .140 | .560 | .112 | .448 | .094 | .376 | .163 | .650 | | | | | .093 | .372 |
| 140 | 432.00 | .138 | .552 | .150 | .600 | | | | | .170 | .680 | .120 | .480 | | | .195 | .780 | | | | | .106 | .424 |
| 150 | 463.00 | | | .160 | .640 | | | | | | | | | | | .245 | .980 | | | | | .135 | .540 |
| 160 | 494.00 | | | | | | | | | | | | | | | .315 | 1.260 | | | | | .145 | .550 |
| 170 | 525.00 | | | | | | | | | | | | | | | | | | | | | | |

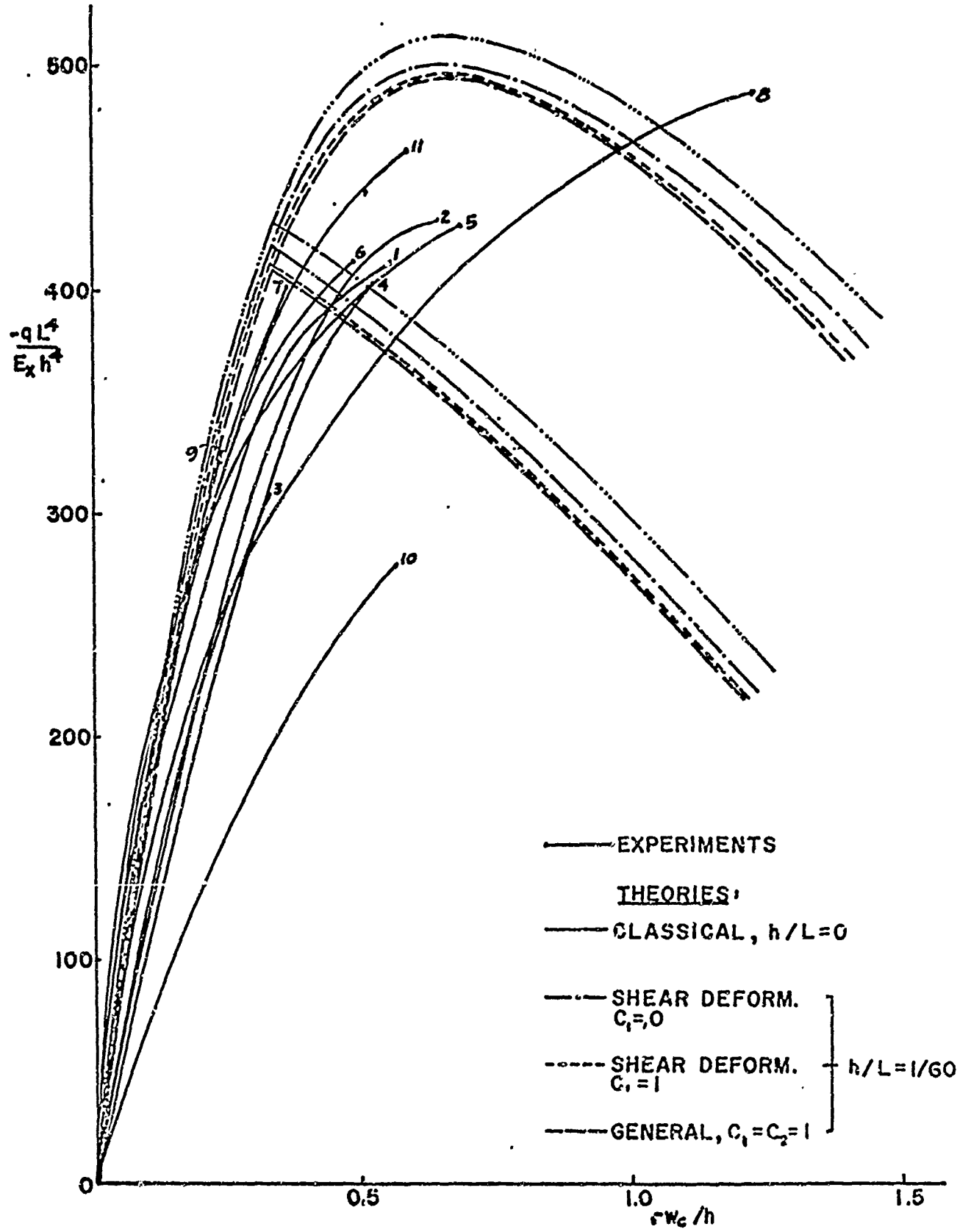


FIG. 15 COMPARISON BETWEEN THEORETICAL & EXPERIMENTAL RESULTS — $\lambda = 56.7$

deflected symmetrically up to approximately 130 $lb/in^2$ but finally buckled into an unsymmetric configuration. Figs. 13(c) and (d) illustrate this arch as progressively greater pressures were applied.

The experimentally obtained arch displacements were usually somewhat greater than predicted by theory. This is attributed to (i) too great a resin content in the mosaic blocks, (ii) nonhomogeneities in the blocks, and (iii) a fully clamped condition was not achieved at the supports.

An overall characteristic of the arches was a slight brittleness. This is not necessarily an inherent property of such a composite material but is believed to be due to impurities or possible dislocations in the specimens.

# CHAPTER V

# CONCLUSIONS

The analytical results obtained from the classical-type theory lead to higher buckling loads than if transverse shear effects are included. Inclusion of transverse normal stress effects in addition to transverse shear still further decreases the predicted buckling loads. The predictions of these three types of theories are in closer agreement as the thickness of the arch decreases.

The transverse normal stress effect on a thin or even a moderately thick arch is small and can usually be neglected. However the effect of transverse shear is quite significant even in the case of a thin arch. For the theory incorporating shear deformation effects the modification in strain-displacement relations achieved by not completely neglecting terms of the form z/R leads to predictions in better agreement with experiments than if these terms are completely neglected.

It was found analytically that the dimensionless parameter $\lambda$ can be used to characterize regions of symmetric and asymmetric buckling. The value of 10.8 for this parameter separates these types of buckling for a hinged end arch and a value of 25 for a clamped end arch.

Predictions of the general theory developed in this study, which includes transverse shear as well as transverse normal stress effects are in satisfactory agreement with experimental evidence and permit reasonably accurate predictions of load-deflection relations of a uniformly loaded arch fabricated of radially reinforced composite material.

## REFERENCES


(1) Timoshenko, S. & Gere, J. M.: Theory of Elastic Stability. Second ed., McGraw-Hill Book Co., Inc., 1961.

(2) Fung, Y. C. & Kaplan, A.: Buckling of Low Arches or Curved Beams of Small Curvature. National Advisory Committee for Aeronautics Tech. Note 2840.

(3) Biezeno, C. B.: Das Durchschlagen eines schwach gekrummten Stabes. Z.a.M.M., Bd. 18. Heft 1, Feb. 1938, pp. 21-30.

(4) Federhofer, Karl: Sitzber Akad Wiss. Wien, 1934 and Bautechnik, No. 41, 1936.

(5) Federhofer, Karl: Dynamik des Bogentragers und Kreisringes, Wein, Springer Verlag 1950.

(6) Friedrichs, K. O.: Lectures on Non-linear Elasticity. Mimeo. notes by S. Schaaf. New York Univ., 1945.

(7) Marguerre, Karl: Uber die Anwendung der energetichen Methode auf Stabilitats probleme. Jahrb. 1938, DVL, pp. 252-262.

(8) Gjelsvik, A. & Bodner, S. R.: Energy Criteria and Snap Buckling of Arches. Journal of Engineering Mechanics Division, ASCE, Vol. 88 No. EM5, Oct. 1962, pp. 87-133.

(9) Schreyer, H. L. & Masur, E. F.: Buckling of Shallow Arches. Journal of the Engineering Mechanics division, Proc. of ASCE, Vol. 92 No. EM4, August, 1966.

(10) Hildebrand, F. B., Reissner, E., & Thomas, G. B.: Notes on the Foundations of the Theory of Small Displacements of Orthotropic Shells. NACA Tech. Note No. 1833.

(11) Green, A. E. and Zerna, W.: The Equilibrium of Thin Elastic Shells. Quart, J. Mech and Applied Math. 3, 9-22 (1950).

(12) Reissner, E.: Stress Strain Relations in the Theory of Thin Elastic Shells. J. Math. Phys. 31, 109-119 (1952).

(13) Naghdi, P. M.: On the Theory of Thin Elastic Shells. Quart. Appl. Math., Vol. XIV, 1956, pp. 369-380.

(14) Love, A.E.H.: A Treaties on the Mathematical Theory of Elasticity. Fourth ed., The Univ. Press (Cambridge), 1934.

(15) Reissner, E.,: The Effect of Transverse Shear Deformation on the Bending of Elastic Plates. Trans. ASME, Vol. 67, 1945, pp A-69 to A-77.

(16) Wilson, P. E.: The Influence of Transverse Shear on the Large Deflection of Elastic Flat Plates. Ph.D. Thesis, Dept. of TAM, U. of Ill., 1961.

(17) Archer, R. R.: A Non-linear Shear Deformation Theory for Thin Elastic Shells. Engineering Research Institute, Univ. of Mass., Tech. Report No. EM 68-1.

(18) Volmir, A. S.: A Translatior of Flexible Plates and Shells. Technical Report AF FDL-TR-66-216, Dept of Eng. Science and Mech., Univ. of Florida, 1967.

(19) Langhaar, H. L.: Energy Methods in Applied Mechanics. John Wiley and Sons, Inc., 1962.

(20) Thurston, G. A.: Newton's Method Applied to Problem in Nonlinear Mechanics. J. of Applied Mechanics, Vol. 32, Series E., No. 2, June 1965.

(21) Reissner, E.: On a Variational Theorem for Finite Deformations. J. Math. and Phys. 32, 1953, pp. 129-135.

(22) Uniroyal, Inc.: Radial Filament Spheres for Deep Submergence Applications, Product Data Sheet No. DD-109.

(23) Elliott, D. R., MacDonald, D. C., Francois, E. Jr., & Uhlig, E. C.: Radial Filament Spheres for Deep Submergence. 12th National SAMPE SYMPOSIUM DS-4.

(24) Nash, W. A. and Hsueh, P. K.: Buckling of Thin Shallow Anisotropic Spherical Shells with a Consideration of Transverse Shear. Scheduled for publication in the proceedings of the International Association of Shell Structures Pacific Symposium, Part I, Honolulu, Hawaii, Oct. 1971.